



KERNFORSCHUNGSANLAGE JÜLICH GmbH

Institut für Reaktorentwicklung

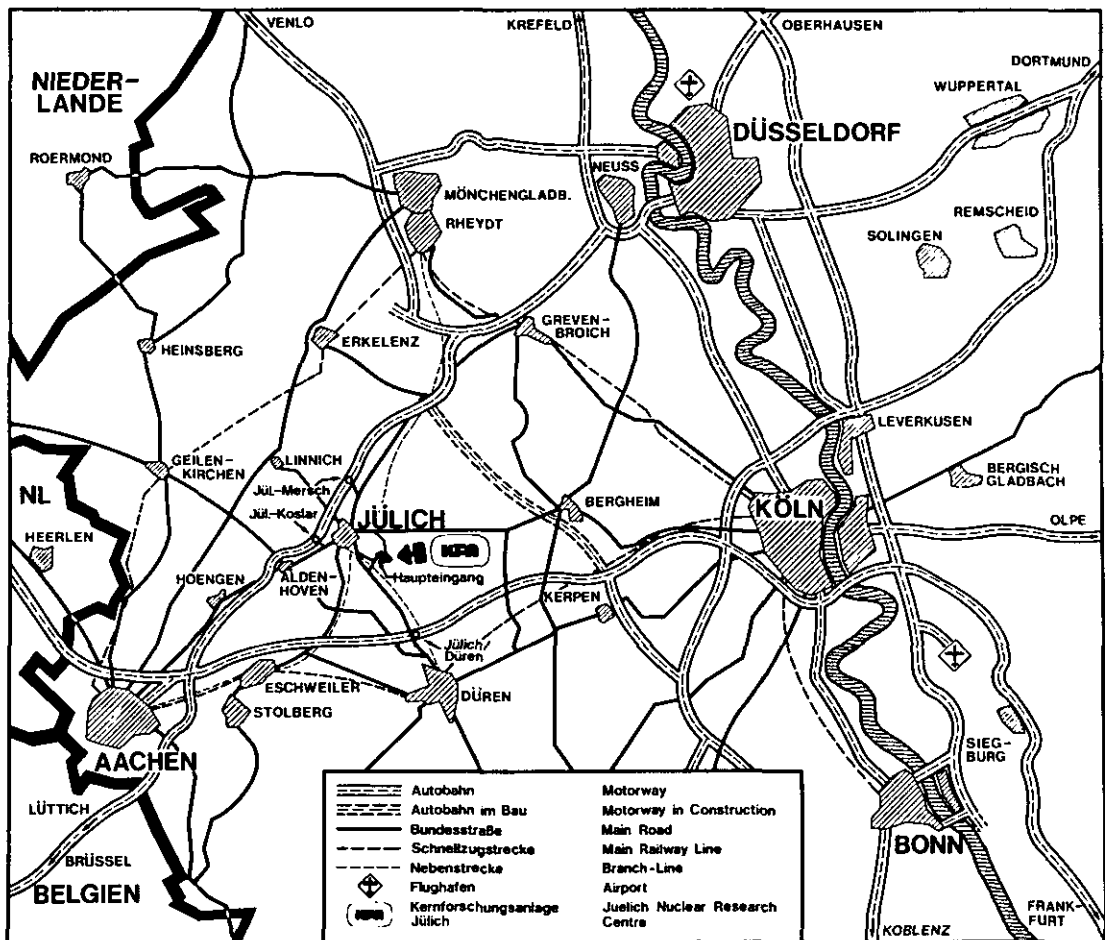
**The Results of Test Run Ia with
the Experimental Facility „AUWARM”**

by

M. Hishida, H. D. Röhrig, J. Schaefer

**Jül - Spez - 23
November 1978**

ISSN 0343-7639



Als Manuskript gedruckt

Spezielle Berichte der Kernforschungsanlage Jülich - Nr. 23
Institut für Reaktorentwicklung J01 - Spez - 23

Zu beziehen durch: ZENTRALBIBLIOTHEK der Kernforschungsanlage Jülich GmbH,
 Jülich, Bundesrepublik Deutschland

**The Results of Test Run Ia with
the Experimental Facility „AUWARM”**

by

M. Hishida, H. D. Röhrig, J. Schaefer

THE RESULTS OF TEST RUN 1A WITH THE
EXPERIMENTAL FACILITY "AUWARM"

by

M. Hishida*
H.D. Röhrig
J. Schaefer

ABSTRACT

The experimental facility "AUWARM" in spite of being designed for hydrogen permeation tests under steam/methane reforming conditions, was also used for studies on the hydrogen permeation under conditions of coal gasification with steam.

As an attempt, specimens were made of a tube which had been exposed in a gas generator, and tested in the facility. The experimental results indicate that in principle good oxide layers establish in a process gas typical for coal gasification with steam, whereas the original scales have probably been damaged by the sample manufacturing.

* delegated from Japan Atomic Energy Research Institute to KFA
Jülich, IRE

DIE ERGEBNISSE DES VERSUCHSLAUFES 1A IN DER EXPERIMENTIERANLAGE "AUWARM"

von

M. Hishida
H.D. Röhrig
J. Schaefer

Kurzfassung

Die Experimentieranlage "AUWARM", die eigentlich für Wasserstoff-Permeationstests unter Bedingungen der Dampf/Methan-Reformierung ausgelegt ist, wurde auch für Untersuchungen zum Wasserstoffdurchtritt unter Bedingungen der Wasserdampf-Kohlevergasung eingesetzt.

Versuchsweise wurden aus einem Rohr, welches in einem Gasgenerator eingebaut war, Proben hergestellt und in der Experimentieranlage getestet. Die Ergebnisse zeigen, daß sich in einem für die Wasserdampf-Kohlevergasung typischen Prozeßgas im Prinzip gute Oxidschichten ausbilden, wohingegen die ursprünglichen Schichten wahrscheinlich schon bei der Probenherstellung stark beschädigt wurden.

CONTENTS

	<u>page</u>
1. INTRODUCTION	1
2. EXPERIMENTAL PARAMETERS	3
3. EXPERIMENTAL RESULTS	5
3.1 Results of Phase-I experiment	5
3.2 Results of Phase-II experiment	7
3.2.1 Explanation of measured data	10
3.2.2 A comparison of the several stages of the oxidation	18
3.3 Summary of the experimental results	19
4. CONCLUSION	23
5. ACKNOWLEDGMENTS	24
List of Tables and Figures	
Table I Experimental parameters	26
Table II Comparison of the process gas composition	4
Table III Temperature changing speed	43
Figure 2.1 Experimental parameters in Phase II experiment	27
Figure 2.2 Concentration of steam and hydrogen gas	28
Figure 3.1 Hydrogen gas concentration in primary Ar gas stream, temperature of test sample, and H ₂ gas pressure	29
Figure 3.2 The dependency of hydrogen permeation on hydrogen pressure (material: Incoloy-800)	30
Figure 3.3 The dependency of hydrogen permeation on hydrogen pressure (material: Incoloy-800)	31
Figure 3.4 The relation between hydrogen permeability and sample temperature	32
Figure 3.5 The dependency of the hydrogen permeation coefficient on the sample temperature (Arrhenius plot of the permeation coefficient)	33

	<u>page</u>
Figure 3.6 Measured hydrogen permeation flux (test sample 106)	34
Figure 3.7 Measured hydrogen permeation flux (test sample 107)	35
Figure 3.8 Measured hydrogen permeation flux (test sample 108)	36
Figure 3.9 Measured hydrogen permeation flux (test sample 109)	37
Figure 3.10 Comparison of the hydrogen permeation rate between 4 test samples	38
Figure 3.11 Hydrogen permeation flux ratio, $J_i/J_{m,i}$ (test sample 106)	39
Figure 3.12 Hydrogen permeation flux ratio, $J_i/J_{m,i}$ (test sample 107)	40
Figure 3.13 Hydrogen permeation flux ratio, $J_i/J_{m,i}$ (test sample 108)	41
Figure 3.14 Hydrogen permeation flux ratio, $J_i/J_{m,i}$ (test sample 109)	42
Figure 3.15 The effect of temperature and time during the exposure to the process gas (Test sample 106)	45
Figure 3.16 The effect of temperature and time during the exposure to the process gas (test sample 107)	46
Figure 3.17 The effect of temperature and time during the exposure to the process gas (Test sample 108)	47
Figure 3.18 The effect of temperature and time during the exposure to the process gas (Test sample 109)	48
Figure 3.19 The comparison of activation energies between 347 stainless steels treated by various methods (10).	49

1. INTRODUCTION

The hydrogen isotopes permeation through reformers, heat exchangers, and gas generators for the gasification of coal, is one of the novel problems in development of Process Heat Systems of High Temperature Gas Cooled Reactors.

Many fundamental and applied studies have been done on the problems (1) (2) (3) (4) (5) (6). Many studies, however, have concentrated up to now on the hydrogen permeation through reformers. Only few studies have been made on the hydrogen permeation through gas generators for the coal gasification with steam.

The process gas outside the gasificating tubes is oxidizing atmosphere, like the one in reforming tubes, as a consequence of the steam surplus in the process gas stream (7) (8). One can expect that the oxide film is built up in an oxidizing atmosphere in the gas generators and thus the hydrogen permeation rate is reduced remarkably in case of gasificating tubes as well as in case of reforming tubes. However, the composition of the process gas in the gas generator is different in the point of percentage from that in the reformer. The hydrogen permeation rates through the oxidized metal are not well understood at present as well as the oxidizing procedure in the high temperature atmosphere. Moreover, the relation between the temperature change (or pressure change) and the damage of the oxide film is not yet established. Therefore, it is necessary to prove, by the experiments, the effect of the oxide film on decrease in the hydrogen permeation and the effect of temperature or pressure changes on damage in the oxide layer, which accompanies the deterioration of the barrier effect of the oxide layer.

In the present experiment, the hydrogen permeation rate of Incoloy-800 was measured in the oxidizing atmosphere simulating the actual process gas in the gas generator for the coal gasification. It

was also observed how the temperature and pressure change affects the permeation rate of Incoloy-800 covered with the oxide layer.

2. EXPERIMENTAL PARAMETERS

The experimental apparatus is described elsewhere (2). The present experiment includes two phases, Phase I and Phase II. In the experiment of Phase I, the hydrogen permeation rate of bare Incoloy-800 was measured with the test sample No. 106. Experimental parameters are listed in Table I. The pressure of pure hydrogen gas was changed in the range of 5 - 10 atm. The temperature of the sample was changed in the range of 450 - 950°C.

In the Phase II experiment, the hydrogen permeation rate was measured with test samples No. 106 - 109. The test samples No. 107 - 109 were made of a gasificating tube, the inside of which had been exposed to the 950°C process gas of the steam gasification of coal for 600 hours. The material of the tube is Incoloy-800. The objectives of the Phase II experiment are as follows:

- (1) To observe the characteristics of the hydrogen permeation of a typical gasificating tube which had been operated in an actual gas generator for a certain period enough to establish an equilibrated oxide film in a practical meaning. Test samples No. 107 - 109 were made from 3 parts of the gasificating tube, namely a lower, a middle and an upper part of the gasificating tube, respectively. It is expected that, corresponding to the tube section, different oxide layers were established and were kept in equilibrium.
- (2) To measure the hydrogen permeation rate of Incoloy-800 in the oxidizing atmosphere simulating the actual process gas in the gas generator.
- (3) To observe the effects of temperature or pressure changes on the damage of the established oxide film.

Experimental parameters, such as temperature of test samples, pressure of the secondary gas circuit and flow rates of supplied water and process gas are shown in Figure 2.1. Partial pressure of hydrogen gas (in the secondary gas circuit) was calculated from the measured values of the total pressure and flow rates

of supplied water and process gas. It was very difficult to keep the total pressure and flow rates at a constant value because of the limited supply of the process gas. Therefore, some small fluctuations in these values were unavoidable. Average values in each scheduled period were taken for the present evaluation.

Figure 2.2 shows the concentrations of steam and hydrogen gas; which were kept at 50% - 70%, and at 15% - 25%, respectively. The concentrations of the gas components in the secondary circuit are listed in Table II, together with actual values in the process gas of gas generators.

The concentrations of hydrogen and steam in the present experiment are almost the same values as the ones of an actual gas generator.

Table II. Comparison of the process gas composition

	process gas at the exit of an actual gas generator	process gas in the present experiment
CO	9.6 %	8.8 - 13 %
CO ₂	4.8 %	4.3 - 6.5 %
CH ₄	0.8 %	0.9 - 1.05 %
H ₂	19.8 %	18 - 27 %
H ₂ O	65 %	53 - 69 %

3. EXPERIMENTAL RESULTS

3.1 Results of Phase-I experiment

Figure 3.1 shows the measured hydrogen permeation rate in terms of concentration in the primary Ar-gas stream, together with the hydrogen gas pressure (P_{H_2}) and the test sample temperature (θ_w). As shown in the figure, the change of the hydrogen permeation rate follows well the temperature and pressure changes.

Figures 3.2 and 3.3 show the dependency of the hydrogen permeation rate on hydrogen pressure. As it is clear in the figures, the hydrogen permeation rate follows the square-root dependency of the hydrogen pressure, which is a characteristic of the bare metal. The hydrogen permeability, P_M , which is the ordinate of Figure 3.2, is defined here as the hydrogen permeation rate through the cylinder of 1 cm^2 in inner area and of 1 cm in effective thickness, t_{eff} , during 1 hour. P_M and t_{eff} are expressed by the following equations (3.1) and (3.2).

$$P_M = \frac{\dot{V}}{\left[\frac{2\pi r_i l}{r_i \cdot \ln r_o / r_i} \right]} = K_M \times \sqrt{P_{H_2}} \times e^{-\frac{Q_M}{RT}} \quad (3.1)$$

$$t_{\text{eff}} = r_i \cdot \ln r_o / r_i \quad (3.2)$$

Here; \dot{V}	: volume flow rate of H_2 through the cylindrical test sample	(Ncc/h)
l	: length of the test sample	(cm)
r_i, r_o	: inner and outer radius of the test sample	(cm)
P_{H_2}	: partial pressure of H_2 gas	(bar)
R	: gas constant = 0.001986	(Kcal \cdot $^{\circ}$ K/mol)
T	: absolute temperature	($^{\circ}$ K)
K_M	: hydrogen permeation constant	(Ncc/h \cdot cm \cdot bar $^{1/2}$)
Q_M	: activation energy for hydrogen permeation	(Kcal/mol)

The effective thickness is equivalent to the thickness of the flat plate.

Figure 3.4 shows in the logarithmic scale the relation between the hydrogen permeability and the reciprocal of the absolute temperature ($1/T$), as a parameter of hydrogen pressure.

Figure 3.5 shows the relation between the hydrogen permeation coefficient and $1/T$. The data points shown by the circle symbol (o) represent the experimental data measured in Phase I experiment. A double circle point (\odot) shows the experimental value measured in the first step of the Phase-II experiment with test sample 106, and with the process gas. As shown in Figure 3.1., the hydrogen concentration measured at 450°C in Phase-I experiment, was slightly decreasing with time. Therefore, the data points at 450°C in Phase-I experiment, shown by the symbol (o), might be affected by the outgassing from the testing unit and might result in a little larger value than the true one. On the other hand, the measurement point represented by a double circle might be affected by a thin oxide layer and might result in a little smaller value than the true one, because the test sample was exposed to Ar gas atmosphere of 450°C - 950°C for 10 days since the end of Phase I experiment until the beginning of the Phase II experiment. During the period, the thin oxide layer might be established by a small amount of O_2 in Ar gas.

A least square method gives the value of 15.5 kcal/mol for the activation energy of Incoloy-800 and the value of $145.6 \text{ Ncc/h}\cdot\text{cm}\cdot\text{bar}^{1/2}$ for the permeation constant. Accordingly, the hydrogen permeation coefficient of Incoloy-800, K_{H_2} , is represented by the following equation (3.3)

$$K_{\text{H}_2} = 145.6 e^{-\frac{15.5}{RT}} \quad (3.3)$$

And the hydrogen permeation rate is expressed by the following equation (3.4).

$$\dot{V} = \frac{2\pi l}{\ln r_o/r_i} \times 145.6 \times \sqrt{p_{H_2}} \times e^{-\frac{15.5}{RT}} \quad (3.4)$$

in the dimension given above.

Present experimental data are somewhat larger than those of other researchers (2) (3) (9). (The experimental point (Δ) of R.A. Strehlow and H.C. Savage (1) was measured with D_2 . The H_2 -permeation coefficient estimated from the data according to the reference (11), is still less than the present data by a factor of 3.)

The difference between the present experimental data and those of other workers might be caused by a little difference in the amount of components added to Incoloy-800, or the difference in the real surface area (roughness) or surface treatment of the samples.

3.2 Results of Phase II experiment

Figures 3.6 - 3.9 show the measured hydrogen permeation rate of test samples No 106-109, in terms of hydrogen permeation flux at the inside surface, J_i ($Ncc/h \cdot cm^2$). In Figure 3.10, a comparison is made between four test samples.

For the purpose of having a better and easier grasp of the phenomena shown in Figures 3.6 - 3.9, the measured hydrogen flux, J_i , was compared with the calculated flux, $J_{M,i}$, through the bare Incoloy-800 tube with the same equivalent thickness, $r_i \cdot \ln r_o/r_i$. The flux ratio, $J_i/J_{M,i}$ is represented by curve (a) in Figures 3.11 - 3.14. In calculating the flux ratio, equation (3.3) was taken as the hydrogen permeation coefficient of bare Incoloy-800.

In the period from 7-th day to 12th day (in the period of temperature change experiment), the hydrogen permeation flux ratios at $950^\circ C$ ($1223^\circ K$) were estimated from the measured data at various temperatures by the following equation (3.5).

The estimated flux ratios, R' , are compared with the asymptotic flux ratio measured at 950°C , for the purpose of observing the effect of temperature changes on the mechanical stability of the established oxide layer.

$$R'(1223^{\circ}\text{K}) = \frac{J_i'(1223^{\circ}\text{K})}{J_{M,i}(1223^{\circ}\text{K})}$$

$$J_i'(1223^{\circ}\text{K}) = J_i(T^{\circ}\text{K}) \times \frac{e^{-\frac{Q'_{ox}}{R \times 1223}}}{e^{-\frac{Q'_{ox}}{RT}}} \quad (3.5)$$

$$J_{M,i}(1223^{\circ}\text{K}) = \frac{K_M \cdot \sqrt{P_{H_2}} \cdot e^{-\frac{Q_M}{R \times 1223}}}{r_i \cdot \ln r_o / r_i}$$

Here, $R'(1223^{\circ}\text{K})$; estimated hydrogen permeation flux ratio at 1223°K
 $J_i'(1223^{\circ}\text{K})$; estimated hydrogen permeation flux at 1223°K
 $J_i(T^{\circ}\text{K})$; measured hydrogen permeation flux at $T^{\circ}\text{K}$
 Q'_{ox} ; apparent activation energy of the oxidated metal
 K_M ; hydrogen permeation constant of bare Incoloy-800
 Q_M ; activation energy of bare Incoloy-800.

In the above equations, it is difficult to assume the proper value for the apparent activation energy of the oxidated Incoloy-800, because it is considered that the apparent activation energy of the oxidated metal differs with the states of oxidation, with the extents of the damage and with the kinds of oxide. For instance, according to the experimental result reported in the paper⁽⁴⁾, the apparent activation energy of the oxidated Incoloy-800, the impeding factor of which is ca. 10^{-2} , is about 8.7 Kcal/mol. On the other hand, the paper⁽⁶⁾ reports that the apparent activation energies of the oxidated Incoloy and oxidated IN materials are 18-23 Kcal/mol. The authors of the report⁽⁶⁾ attribute the metallic behaviour in the apparent activation energy to the presence of small imperfections in the oxide film. According to the experiments of the report⁽¹⁰⁾, the activation energy of the 347 stainless steel oxidated by the wet hydrogen gas at 979°C is about 16 Kcal/mol which is almost same as the one of the pure 347 stainless steel (15 Kcal/mol) (see Figure 3.19). And the activation energies of the 347 stainless steel coated by

various oxides are 13 Kcal/mol-19 Kcal/mol. These results⁽⁴⁾
(6) (10) seem to indicate that the apparent activation energy
of the oxidated metal spreads in the wide range, depending
on the kinds of the oxide, states of the oxidation and the
extents of the damage in the oxide film. In the present evaluation,
the flux ratios, R' , were estimated for activation energies of
5 Kcal/mol, 10 Kcal/mol, 15 Kcal/mol and 20 Kcal/mol. They are
represented in Figures 3.11 - 3.14 by curves (A), (B), (C) and
(D) respectively. Naturally, curve (C) almost coincides with curve
(a).

3.2.1 Explanation of measured data

As shown in Figure 3.10, the hydrogen permeation behaviour measured with test sample No 106 is somewhat different from those measured with No 107-109, while the behaviours of test samples No 107-109 are very similar to one another. The difference between No 106 and No 107-109, especially the difference after 2nd day, seems to depend upon the difference in the oxide layers established during the present experiment. The measured results of the test samples are described as follows. (Refer to Figures 3.6-3.9 and Figures 3.11-3.14).

At the first step of the experiment, hydrogen permeation rates were measured at the relatively low temperature of 450°C. For the purpose of measuring the permeation rate through test samples 107-109 without further oxidation, process gas of relatively low temperature was led into the samples.

The hydrogen permeation rate went up gradually and reached an asymptotic value. After that, any increasing or decreasing in the hydrogen permeation rate was not recognized. It means that at the sample temperature of 450°C, an oxidation speed was so slow that the hydrogen permeation rate remained at a constant value. The asymptotic values of the hydrogen flux ratio of test samples No. 107-109 lay in the range of 0.1-0.4. This means that some extent of oxide film had been established inside the test samples by a preceding exposure in a gas generator. But the flux ratio, $J_i/J_{M,i}$, (or the diminished rate of the hydrogen permeation) was not so small as the one attained by the subsequent experiment. Judging from the relatively high value of $J_i/J_{M,i}$, the oxide layer which had been established in an actual gasificating tube, seemed to be almost damaged. The damage in the oxide film might have been caused by the shut-down at the end of the operation or caused by the manufacturing process in making test samples from a gasificating tube (for instance cutting, machining, welding etc.) This introduces so many uncertainties that the differences in the flux ratios are easily understood. The asymptotic value of the hydrogen flux ratio of test sample 106 was about 0.7, which would be explained by the thin oxide film established before the Phase II experiment, as mentioned before.

(see chapter 3.1)

After the asymptotic hydrogen permeation rate was measured, the sample temperature was raised to observe the effect of oxidization on the hydrogen permeation. As shown in Figures 3.6-3.9, the hydrogen permeation rate increased with the temperature rise and after the temperature had reached a constant value of 800°C , it turned to a steep decrease. It is not clear in Figures 3.6-3.9, whether the initial steep increase in hydrogen permeation rate was caused only by the temperature dependency of the hydrogen permeation or not. But from Figures 3.11-3.14, it is evident that the increase in hydrogen permeation resulted only from the greater permeability accompanied by the higher sample temperature and not from the damage in the oxide-film.

The subsequent sharp decrease in the permeation rate is accounted for the build-up of a new oxide film inside the test samples. Because of the higher temperature of 800°C , the oxidization proceeded rapidly. The permeation ratio became less than 1/100 after 40 hours' operation.

The decreasing speed varied with test samples. And moreover, in case of test sample No. 107, the decreasing speed increased almost abruptly 18 hours after the beginning of the oxidization, in spite of the constant experimental condition. The reasons for the different decreasing speeds for the samples and for the abrupt change of the decreasing speed of No. 107 are not clear. But these experimental facts seem to indicate that the oxidation procedure is very complicated and is affected by many factors, for instance a little difference in material, the surface treatment of a test sample, existence of small amounts of impurity gases and other unknown factors.

At the next step, the sample temperature was raised up to 950°C . The permeation rate was increased stepwise with the temperature rise. It can be said, this increase was also caused only by the temperature dependency of the hydrogen permeation and not caused by some defects in oxide layer, as it is clear in Figures 3.11-3.14.

After the constant temperature of 950°C had been attained, the hydrogen permeation rate again fell down steeply. It appears that, because of the higher temperature, the oxidization speed was greater than before, and this resulted in a higher decreasing

rate of the hydrogen permeation rate. Seven days after the beginning of Phase-II experiment, the flux ratios, $J_i/J_{M,i}$ of all the 4 samples reached the asymptotic values of 10^{-3} - $2 \cdot 10^{-3}$.

At the 4.6 th day, the hydrogen partial pressure was lowered to 0.84 bar (it corresponds to 4.9 bar of the total pressure) from 1.84 bar (total pressure: 9.81 bar). And at the 5.5 th day, it was raised up to 2.44 bar (total pressure: 9.81 bar). Corresponding to the lower and higher partial pressure, the hydrogen permeation rate decreased and increased. Flux ratios estimated by the assumptions that the permeation rate of oxide film depends on the square root of P_{H_2} and 1st power of P_{H_2} are shown in Figures 3.11-3.14 by the solid line and the dotted line, respectively. Both lines (values) seem to be discontinuous to the lines (values) that come before and after. But it does not seem to indicate that the oxide film was damaged by pressure changes. As shown in Figures 3.6-3.9, the hydrogen permeation rate changed continuously with the pressure change. And moreover, the permeation rate at $\theta_W = 950^\circ\text{C}$ and $P_{H_2} = 2,44$ bar seems to lie on an extrapolated curve of $\theta_W = 950^\circ\text{C}$ and $P_{H_2} = 1.84$ bar. These indicate that the oxide film was not damaged by the pressure changes. It is considered that a fairly long time is necessary to get an equilibrium in concentrations of gas components when the secondary gas pressure is changed as well as the new equilibrium on the downstream side. This seems to be a reason for the discontinuity of the curves (values), immediately after the pressure changes. In the next step of the experiment, the temperature was changed between 950°C and 500°C to observe the effect of temperature change on the oxide layer.

At first, the temperature was lowered from 950°C to 500° by five steps. The decreasing speed and the extent of temperature drop in each step are written in Table III.

The following experimental facts indicate that the oxide layers of test samples 107-109 were affected by almost every step of temperature drop.

- 1) The hydrogen permeation fluxes measured at 950°C after the temperature change experiments (denoted by (10) in Figures 3.7-3.9) is higher than the asymptotic value measured at 950°C before the temperature change experiments (the asymptotic value denoted by (3) in Figures 3.7-3.9). And the permeation

flux denoted by (10') decreased to almost the same asymptotic values as before, by the subsequent operation at 950°C. This resulted from the annealing effect of the damaged oxide layer.

- 2) The permeation fluxes of 800°C measured at increasing temperature steps (denoted by data points (9') or (10)) is higher than those of 650°C measured at decreasing temperature steps. (denoted by (4)).

The permeation flux at 650°C measured at increasing temperature steps (denoted by data points (8') and (9)) is higher than those measured at the same temperature at decreasing temperature steps. (denoted by data points (4') or (5))

- 3) The oxide layers seemed not to be damaged by the temperature increase from 500°C to 950°C, because,

(I) Arrhenius plots (Figures 3.16-3.18)¹⁾ show that the data points measured during the temperature increase steps fit fairly well the straight lines (see the dotted curves (a) in Figures 3.16-3.18).

(II) In every step of temperature increase, the measured hydrogen flux decreased after the temperature had been kept constant. Any increase in the hydrogen flux, which seems to indicate the occurrence of the damage as described in (6), was not recognized after any step of temperature rise.

Accordingly, it is considered that the experimental facts 1), 2) indicate that the oxide layers were damaged at the temperature decrease steps and not damaged at the temperature increase steps.

- 4) The permeation flux measured at 800°C (denoted by (4) in Figures 3.7-3.9) is almost the same as or higher than the permeation flux measured at 950°C, (denoted by (3)). This means that the oxide layers were damaged by the temperature drop from 950°C to 800°C.

- 5) The estimated flux ratios, R' , denoted by curves (A), (B), (C) show the higher values than the asymptotic values at 950°C measured before the temperature change experiments. (Curve (D) represents the flux ratio estimated by the assumption that the activation energy of the oxidated metal is 5 Kcal/mol. As discussed later, the assumed activation energy of 5 Kcal/mol seems not to be realistic in the present experiment).

1) Figures 3.15-3.18 are also referred to in another connection later on.

- 6) In most cases of temperature drop, the hydrogen flux increased continuously over 5-10 hours after the temperature had been kept at constant values. (for example, in the temperature drops from 950°C to 800°, from 600°C to 550°C in test sample 107, in the temperature drop from 800°C to 650°C in test sample 108, in the temperature drops from 800°C to 650°C, from 650°C to 600°C in test sample 109)

It is not attributed to the time lag which is necessary for getting the steady state of hydrogen permeation, unless the damages are newly created by the temperature drops. For, when the oxide layer is not newly damaged by the temperature drop, the effect of the time lag must decrease the measured hydrogen flux continuously and gradually, even if the oxide layer contains defects before the temperature decrease.

And the outgassing from the testing unit did not appear to be the cause for the continuous increase of hydrogen flux after the temperature drops, because in some cases of temperature drop, the permeation flux was not changed after the temperature had been kept at a constant value.

On the other hand, the following experimental facts indicate that the oxide layer of test sample 106 remained nearly undamaged during the temperature changes.

- 1) The hydrogen flux of 950°C measured after the temperature change (denoted by (10) in Figure 3.6) is almost the same as the asymptotic value at 950°C measured before the temperature change experiment. (denoted by datum point (3))
 - 2) No significant decrease in the permeation flux was recognized after the temperature was raised up to 950°C.
 - 3) The flux ratios represented by curves (A), (B), (C) are smaller than or almost equal to the asymptotic value measured at 950°C.
- However, judging from the fact that the permeation rate decreased slightly when the temperature was afterwards raised up from 650°C to 800°C, it is supposed that the oxide layer was damaged to some extent by several preceding steps of temperature drop or a farther improvement was initiated by some other effects. Anyhow, the extent of damage must have been very small. And it can be said that in a practical sense the oxide layer was not damaged by the temperature drop.

The difference between the result of test samples 106 and that of 107-109 could be caused by a little difference of the material and the difference in surface treatment of the samples. Presumably the oxide film grown on the bare metal under the smooth conditions of Ar plus traces of O_2 (see Phase I) yield the conditions for the build-up of better oxide scales in Phase II. But the full explanation is not found. As mentioned before, the oxide layers of test samples 107 to 109 were damaged by the temperature drops. However, the extent of damage (or the extent of increase in the permeation rate) differed with test samples and with the cases of temperature drop. For instance, the flux ratio of test sample No. 107 became ca. 5 times as large as before by the temperature drop from $950^{\circ}C$ to $800^{\circ}C$, while the one of No. 109 became only ca. 2 times as large. In the present experiment, no definite relations were found between the extent of damage and the magnitude of the temperature drop or the cooling rate of the test samples.

An interesting experimental fact is that the hydrogen permeation rate continued to increase even after the temperature of the test samples was kept at a constant value. Although each experimental period of a constant temperature was not long enough to get an asymptotic permeation rate, 4 - 14 hours were necessary at least to get an asymptotic value of the permeation rate. The following reasons might be a possible explanation for the above phenomena. One of them is as follows.

Defects in oxide layer consist of many cracks. The cracks are supposed to be very small in size or to maldistribute in some local parts of a test sample. Accordingly, when the cracks are newly created by the temperature drops, it takes a fairly long time for the hydrogen concentration to reach a new steady state distribution in a metal, and thus it takes a long time for the measured hydrogen flux to be in a steady state. The alternative possible reason is that an oxide layer is damaged not only during the transitional period of a temperature drop, but also during a subsequent period of constant temperature.

If the latter reason is true, it is an important indication that the oxide layer is damaged not only by the elastic break down caused by the difference in the thermal expansion coefficient

between an oxide film and a base metal. Extensive studies should be done on this point.

During the temperature change experiments, the estimated flux ratios were calculated for four different assumed activation energies of the oxidated metal, and are shown in Figures 3.11-3.14, as mentioned before. In the present experiments, the apparent activation energy of the oxidated Incoloy-800 seems to be at least in a range from 10 to 20 Kcal/mol, by the following reasons.

- (1) The oxide layer of test sample 106 was nearly undamaged by the temperature changes. It means that the value of the estimated flux ratio should not be changed by temperature changes. Curve (B) seems to satisfy the above terms best among the curves. (in every curve, the estimated flux ratio decreased, after the temperature was lowered to 800°C. It might be caused by the further oxidation, although the reason for the further oxidation is not clear. Accordingly, the estimated flux ratio should be the same value at least from the beginning of the temperature drop to 650°C to the end of the temperature change experiment).
- (2) In curves (D) of all the test samples, the values of the estimated flux ratio just after the temperature drops are smaller than the values just before the temperature drops. It should mean that the oxide layers were improved by the temperature drops. But, it is unrealistic.
- (3) There are some cases in which the oxide layers seemed not to be damaged by the temperature drops (for examples, temperature drop from 800°C to 650°C in test sample 107, temperature drop from 550°C to 500°C in test sample 109). And, it is considered that the oxide layers were not damaged by the temperature increase. The experimental data in these temperature drops and increase give ca. 15 Kcal/mol as the apparent activation energy of the oxide layer.

In Figures 3.11 - 3.14, it is clear that the permeability of Incoloy-800 with an oxide layer is ca. 10^{-2} times as small as that of bare Incoloy-800, even though the oxide layer is damaged to some extent by many temperature drops. It means that a naturally

established oxide layer is effective in decreasing (controlling) the hydrogen permeation rate of actual gasificating tubes under normal operation conditions by a factor of ca. 10^{-2} .

After the sample temperature had been lowered to 500°C , it was again increased as far as 950°C by three steps. In any step, the hydrogen permeation rate initially increased stepwise on account of the temperature dependency of the permeation rate; and after the constant temperature was attained, the permeation rate decreased. That resulted from the annealing effect of the higher temperature on the damaged oxide layer.

It is expected that, the higher the sample temperature is raised up, the more is the speed of the subsequent decrease in the hydrogen permeation rate by the farther corrosion rate. And it is also expected that the more the extent of an initial damage is, the faster the permeation rate decreases with the subsequent temperature rise. However the only distinct result which was observed in the present experiment was that the hydrogen permeation rates of test samples 107 - 109 decreased at the highest speed when the temperature was raised up to 950°C .

The hydrogen partial pressure was lowered to 0.94 bar from 2.44 bar about 20 hours after the sample temperature had reached 950°C . It can be said that no damage in the oxide layer was brought about by this pressure change like in the former case when the partial hydrogen pressure was lowered to 0.84 bar from 1.84 bar. The hydrogen permeation rate reached an asymptotic value about 30 hours after the sample temperature was kept at 950°C . The asymptotic flux ratio $J_i/J_{M,i}$ was around 10^{-3} , which was almost the same value as the one at $\theta_w = 950^{\circ}\text{C}$ and $P_{\text{H}_2} = 2.44$ bar.

At the final procedure of the experiment, the temperature was again decreased from 950°C to 800°C . The present behaviour of measured hydrogen permeation of the test samples 107 - 109 is quite different from that of the former temperature drop from 950°C to 800°C with the same decreasing speed of temperature. In the former case, the permeation rate began to increase steeply just after the sample temperature was lowered to 800°C . On the

contrary, a little decrease in the hydrogen permeation was observed in the present case, even after the temperature was kept at 800°C. Though the permeation rate increased by a small amount about 6 hours later, it soon started to decrease slightly. The suitable explanation cannot be given for the differences between both cases. The following reason might be a possible explanation.

In particular experiments in which the magnitude of the temperature change lies within some limits, it might be possible that the oxide layers, as a whole, are hardly to be damaged by the temperature changes after the second time of temperature change. Because, the most parts of the oxide layer which are weak against the thermal stress or induce the stress concentration, have been damaged by the first temperature drop. Many studies will be necessary on this point.

Lastly, the sample temperature was lowered from 800°C to 650°C. In this case, the established oxide layers of $10^7 - 10^9$ were continuously affected over several hours after the temperature drop. But, the extent of damage seems to be smaller, compared with the former temperature drop to 650°C.

3.2.2 A comparison of the several stages of the oxidation

Another representation of the results discussed above, which is often thought to be more perceptual, can be given in the form of Arrhenius diagrams, figures 3.15-3.18. They reveal the several stages of oxidation as compared to each other and to the bare metal. The highest curves in the figures represent the hydrogen permeation flux of the bare Incoloy-800. Several oxidation stages are demonstrated by the curves (I)-(V), and the group of data points (IV). By the exposure to the process gas of 800°C-950°C, the initial stage of the oxide layers were further oxidized and they reached the final stage of the oxide films (curve (III)) through the intermediate stage (curve (II)). In the present experiment, it took 90 - 170 hours for the initial stage of the oxide films to reach the last stage of the oxide films. The permeation flux of the last stage of the oxide films was about 10^{-3} times smaller than that of the bare Incoloy-800. In the last stage, the oxide layers were damaged by the several steps of the

temperature drop, and the permeation flux became a little higher. This stage of the oxide layers is represented by the data group (IV).

The damaged oxide layers were annealed by the operation at higher temperatures. And the permeation rate again decreased to almost the same value as the last stage of the oxide layer (represented by curve (V)).

3.3 Summary of the experimental results

The experimental results stated in the preceding chapters can be summarized as follows;

- (1) At first, an experiment was done to observe the characteristics of the hydrogen permeation of a gasificating tube which had been exposed to an actual process gas of coal gasification for some period enough to establish a so-called equilibrated oxide film inside the tube. The hydrogen permeation rate was measured at 450°C with test samples No. 107 - 109. The measured hydrogen permeation rate was only 0.1-0.4 times as small as that of bare Incoloy-800. Judging from the measured data in the subsequent experiments, it is not considered that the above result represents the hydrogen permeation characteristics of a typical gasificating tube having been operated in an actual gas generator.

The experimental result seems to be affected markedly by fatal damages in the pre-oxidized layer which was build in an actual gas generator. It seems that the damages were brought about in the procedure of manufacturing the test samples.

- (2) The hydrogen permeation data of test samples 107 - 109 measured after 2nd day, were mainly influenced or controlled by the newly established oxide layers and were hardly affected by the pre-oxidated layers.

This can be approved by the following experimental facts.

(I) It appears that the pre-oxidized layer of No. 107-109 was largely damaged before the experiment.

(II) The hydrogen flux of No. 107-109 measured in the period from 2.2th day to 8th day, coincided fairly well with

that of No. 106. Difference in the magnitude of the hydrogen flux between No. 106 and No. 107-109 is within a factor of 2.

- (III) The least asymptotic value of the flux ratio, $J_i/J_{M,i}$ of No. 107 - 109 was about 10^{-3} , which was nearly the same as the least asymptotic value of No. 106 (10^{-3}).
 - (IV) The asymptotic flux ratio of No. 107-109 at $\theta_w = 950^\circ\text{C}$ was the same value before and after the oxide layer was damaged and re-established.
 - (V) The hydrogen flux of No. 106 during the period from 9th day to 12th day, was less than those of No. 107-109.
- (3) Accordingly, the difference of measured hydrogen flux between test sample 106 and test samples 107 - 109 was mainly attributed to the oxide layers newly established during the present experiment. The difference of the surface treatment and possibly a little difference in components of Incoloy-800 seemed to cause the differences in the oxide layer between test sample 106 and test samples 107 - 109.
 - (4) A 40 hours' operation at the temperature of 800°C decreased the hydrogen permeation rate of No. 107-109 to $7 \cdot 10^{-3}$ - $1 \cdot 10^{-2}$ times as small as the one of bare Incoloy-800. (It corresponds to 1/15 - 1/50 times the value of the initial permeation rate). And it was still decreasing. The additional 50 - 100 hours' operation at the temperature of 950°C decreased the flux ratio, $J_i/J_{M,i}$, to an asymptotic value of ca. $1 \cdot 10^{-3}$. (It corresponds to 1/100 - 1/400 times the value of the initial permeation rate).
 - (5) The hydrogen permeation rate of No. 106 decreased to 10^{-2} times the value of the bare Incoloy-800, after 40 hours' operation at 800°C . And the subsequent 50 hours' operation brought it to an asymptotic value which was $2 \cdot 10^{-3}$ times as small as the permeation rate of bare Incoloy-800.
 - (6) Above experimental results (4), (5) lead to the conclusion that the oxide film is built up on the process gas side of actual gasificating tubes.

- (7) Experiments were made to observe the effect of the temperature drop on the established oxide layer. In the first case, the temperature was lowered to 500°C from 950°C by five steps, with the decreasing speed of temperature of 50-150°C/hour and in the second case, it was lowered to 650°C by 2 steps with the same decreasing speed.

The first temperature drop resulted in an increase in the hydrogen flux ratio, $J_i/J_{M,i}$, of test samples Nr. 107-109 by a factor of 5 - 30. In the second case, the flux ratio of No. 107-109 increased by a factor of ca. 2. It appears that the increase in the hydrogen permeation was caused by the damages in the established oxide layer. In spite of the damage in the oxide layer, the flux ratio, $J_i/J_{M,i}$, was less than ca. 10^{-2} . On the contrary the flux ratio, $J_i/J_{M,i}$, of No. 106 did not increase in both cases of temperature drop. The experimental facts lead to a beneficial conclusion that the naturally established oxide layer is effective in decreasing the hydrogen permeation rate of the coal gasification tubes even under realistic operational conditions.

- (8) After the oxide layer was damaged by the temperature decreases, the temperature was again raised up to 950°C by 3 steps to observe the recovering effect of the temperature rise on the damaged oxide film. The temperature rise was accompanied by a decrease in the hydrogen permeation of No. 107-109 and after 30 hours' operation at 950°C, the flux ratio again decreased down to the asymptotic value of ca. 10^{-3} . That is the annealing effect of the damaged oxide layer.

- (9) In the present experiment, oxide scales were not damaged by the pressure changes.

- (10) The following experimental facts which were observed in the present experiment indicate the complexity of the oxidizing mechanism and of damaging mechanism of the oxide film.

(I) The hydrogen permeation flux of all the four test samples decreased steeply when the temperature was raised up to 850°C for the first time. The decreasing speed of hydrogen permeation varied with the samples. Moreover, the decreasing

speed of the permeation flux of test sample 107, changed 18 hours after the beginning of the oxidization, in spite of the constant experimental condition.

- (II) As mentioned in (7), it appears that the oxide layer was damaged by the temperature decrease. The present experiment indicates that the extent of the damage was not determined only by the extent of temperature drop and the decreasing speed of temperature. For instance all the flux ratios, $J_i/J_{M,i}$, of test samples No. 107-109, increased in the first case of temperature drop from 950°C to 800°C, while they decreased slightly in the second case of temperature drop from 950°C to 800°C. Although the flux ratio, $J_i/J_{M,i}$, of No. 107-109, increased by the temperature drops from 950°C to 500°C, the flux ratio of 106 did not increase.
- (III) The permeation flux of test sample 106 continued slightly to increase after the temperature was raised up to 950°C at 11th day. And later, it abruptly turned to decreased in spite of the constant experimental condition.

4. CONCLUSION

1. The measured hydrogen permeability of the bare Incoloy-800 was represented by the following equation.

$$\dot{V} = \frac{2\pi l}{l \ln r_o/r_i} \times 145.6 \times \sqrt{p_{H_2}} \times e^{-\frac{15.5}{RT}} \quad (\text{Ncc/h})$$

2. Gasificating tubes are oxidized in the process gas of gas generators as well as the reforming tubes are oxidized in the atmosphere of reformers. The established oxide film reduces the permeation rate by more than two orders of magnitude.
3. The hydrogen permeation rate decreased to ca. 10^{-2} times the value of bare Incoloy-800, after 40 hours' operation at 800°C in the gas stream simulating the actual process gas of gas generators. By the additional 50 - 100 hours' operation, at the temperature of 950°C it decreased to an asymptotic value of ca. 1×10^{-3} as small as that of bare Incoloy-800.
4. The oxide films of test samples No. 107 - 109 were damaged by the temperature decreases. The hydrogen permeation rate, however, remained still less than ca. 10^{-2} times the value of bare Incoloy-800.

On the other hand, the oxide film of test sample No. 106 remained almost undamaged by the temperature decrease.

5. Though the permeation rate is increased by the damage of the oxide layer, it is again reduced by the subsequent temperature rise. This is caused by the annealing effect of the temperature rise on the damaged oxide layer.
6. It is considered to be of remarkable interest of prove the statements gained from the permeation measurements by proper metallurgical investigations at the samples used and to compare with specimens which had only been exposed in the coal-gasifier.

5. ACKNOWLEDGMENTS

The authors acknowledge their indebtedness to Prof.Dr.R.Hecker, the director of the "Institut für Reaktorentwicklung der Kernforschungsanlage Jülich", who made this investigation possible. And the authors wish to express their appreciation to the members of our group, who made a successful performance of the experiments. Particular thanks are due to Mr.W.Diehl and to Mr.A.Tauber.

Last not least the authors want to thank especially their colleagues in the "Institut für Bergbau-Forschung, Essen" for initiating this investigation and delivering the test samples and the dry process gas.

REFERENCES

- 1 R.A. Strehlow and H.C.Savage, Nucl. Technol., 22 (1974) 127
- 2 H.D.Röhrig, J.Blumensaat and J.Schaefer, Proc. BNES Conf. on the HTR and Process Applications, London, November 1974, British Nuclear Energy Society, Thomas Telford, London, 1975
- 3 Y.Mori and T.Nakada, BNES Conf. on the HTR and Process Applications, London, November 1974, British Nuclear Energy Society, Thomas Telford, London, 1975
- 4 H.D.Röhrig, R.Hecker, J.Blumensaat and J.Schaefer, Nucl. Eng. Des., 34 (1975) 157
- 5 J.Blumensaat, J.Lambrecht, H.D.Röhrig and J.Schaefer, Reaktortagung des DATF/KTG, Mannheim, 1977
- 6 H.D.Röhrig, R.Hecker, Thin Solid Films, 45 (1977) 247
- 7 H.Jüntgen and K.H. van Heek, Nucl.Eng. and Design, 34 (1975) 59
- 8 P.P.Feistel, R.Dürrfeld, K.D.van Heek and H.Jüntgen, Nucl. Eng. and Design, 34 (1975) 147
- 9 J.Blumensaat, Private communication
- 10 P.S.Flint, KAPL-659, Knolls Atomic Power Laboratory, Schenectady, New York, December 14, 1951
- 11 R.Gibson, P.M.S.Jones, J.A.Evans, AWRE 0-47/65 1965

Table I: Experimental Parameters

	Phase I	Phase II
No of test sample	106	106,107,108,109
Material of test samples	Incoloy-800 Composition of Incoloy-800 ⁽⁶⁾ Cr; 19-23%; Fe; 37-45% Ni; 30-35%; Ti; 0.15-0.6% Mn; 1.5% : Al; 0.15-0.6% Si; 1.0% : C ; 0.1%	
Dimensions of test samples	No. 106 149 mm x 48.2 mm ^{o.D.} x41.2mm ^{i.D.} No. 107 150.5mm x48.2 mm ^{o.D.} x41.2mm ^{i.D.} No. 108 150 mmx48.2mm ^{o.D.} x41.2 mm ^{i.D.} No. 109 150 mmx48.2mm ^{o.D.} x41.2 mm ^{i.D.}	
Primary gas circuit		
primary gas	Ar	Ar
flow rate	100 cc/min	100 cc/min
pressure	~ 1 bar	~ 1 bar
Secondary gas circuit		
secondary gas	H ₂	process gas
gas pressure	5~10 bar	5~10 bar
H ₂ partial pressure	5~10 bar	0.8~2.5 bar
Temperature of test sample	450 ^o C~950 ^o C	500 ^o C~950 ^o C

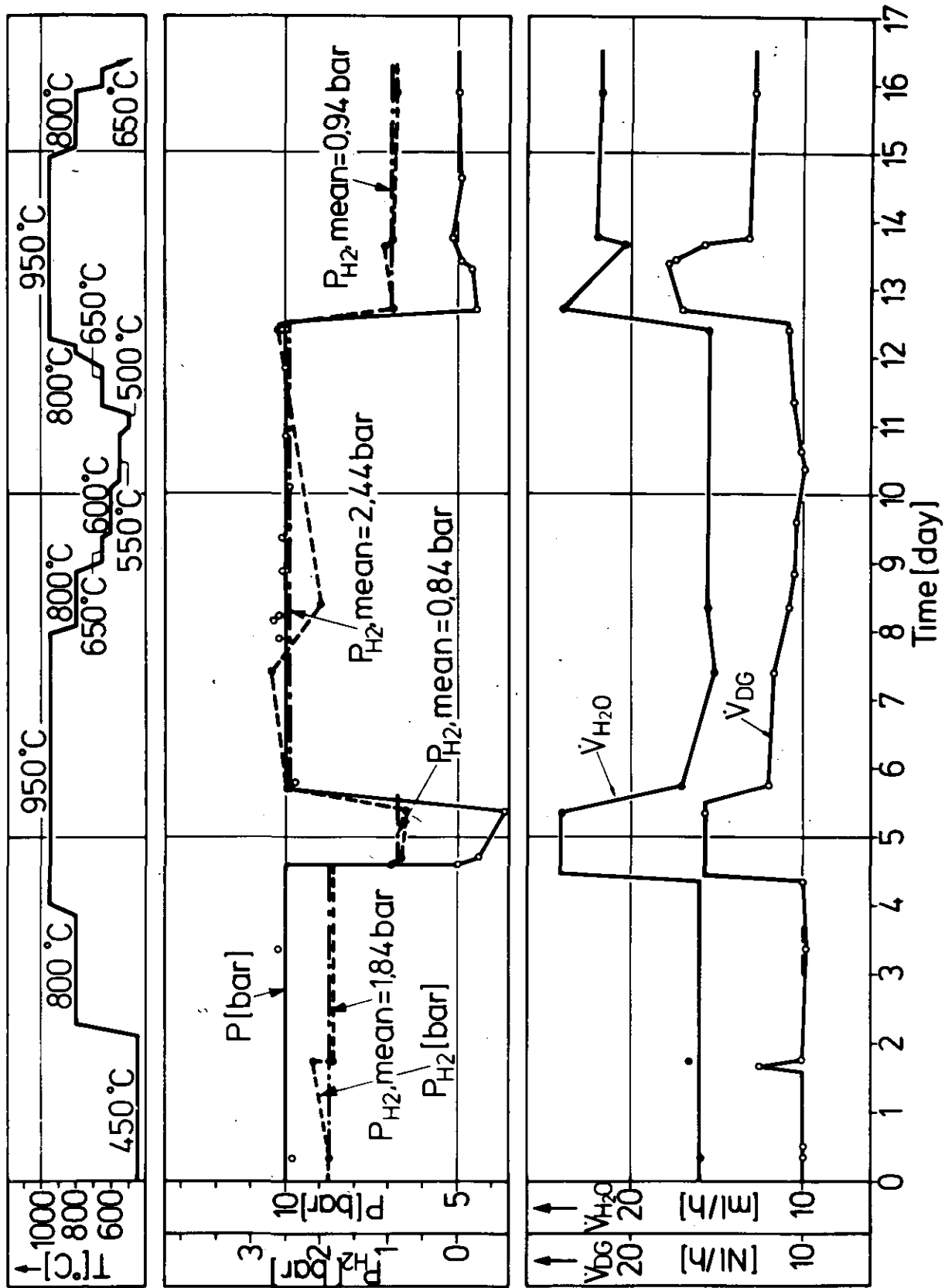


Figure 2.1 Experimental parameters in Phase II experiment

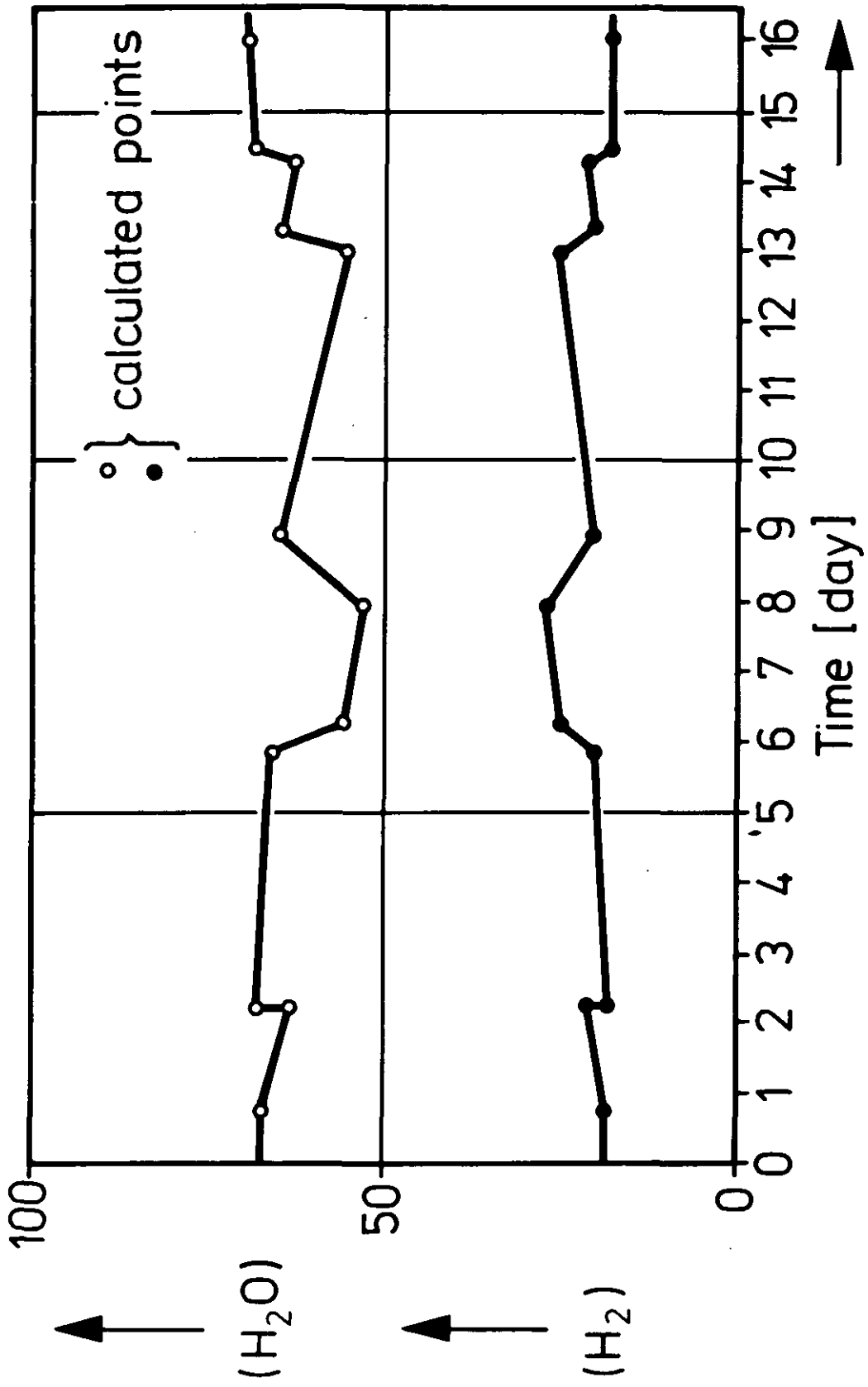


Figure 2.2 Concentration of steam and hydrogen gas

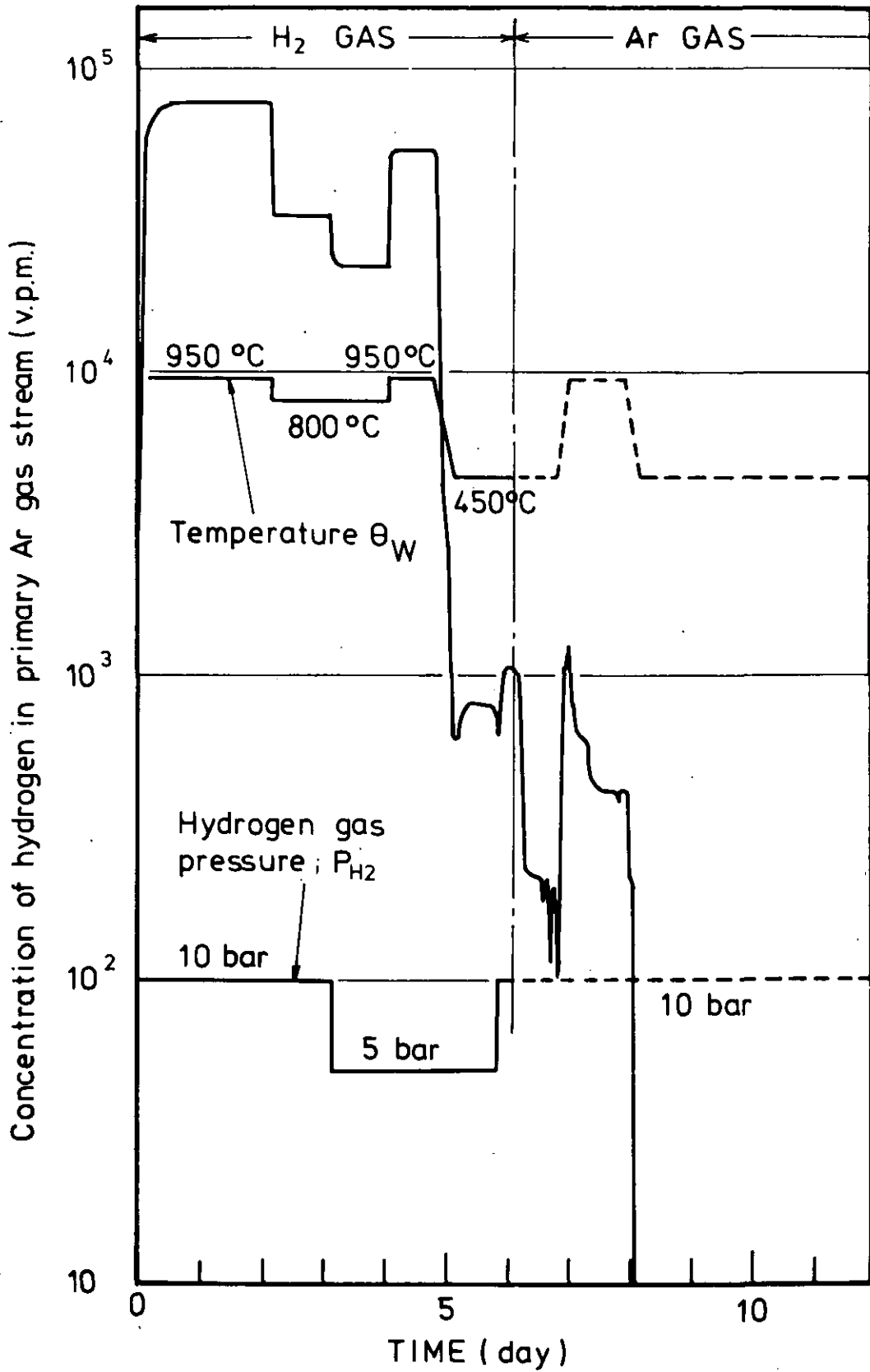


Figure 3.1 Hydrogen gas concentration in primary Ar gas stream, temperature of test sample, and H₂ gas pressure

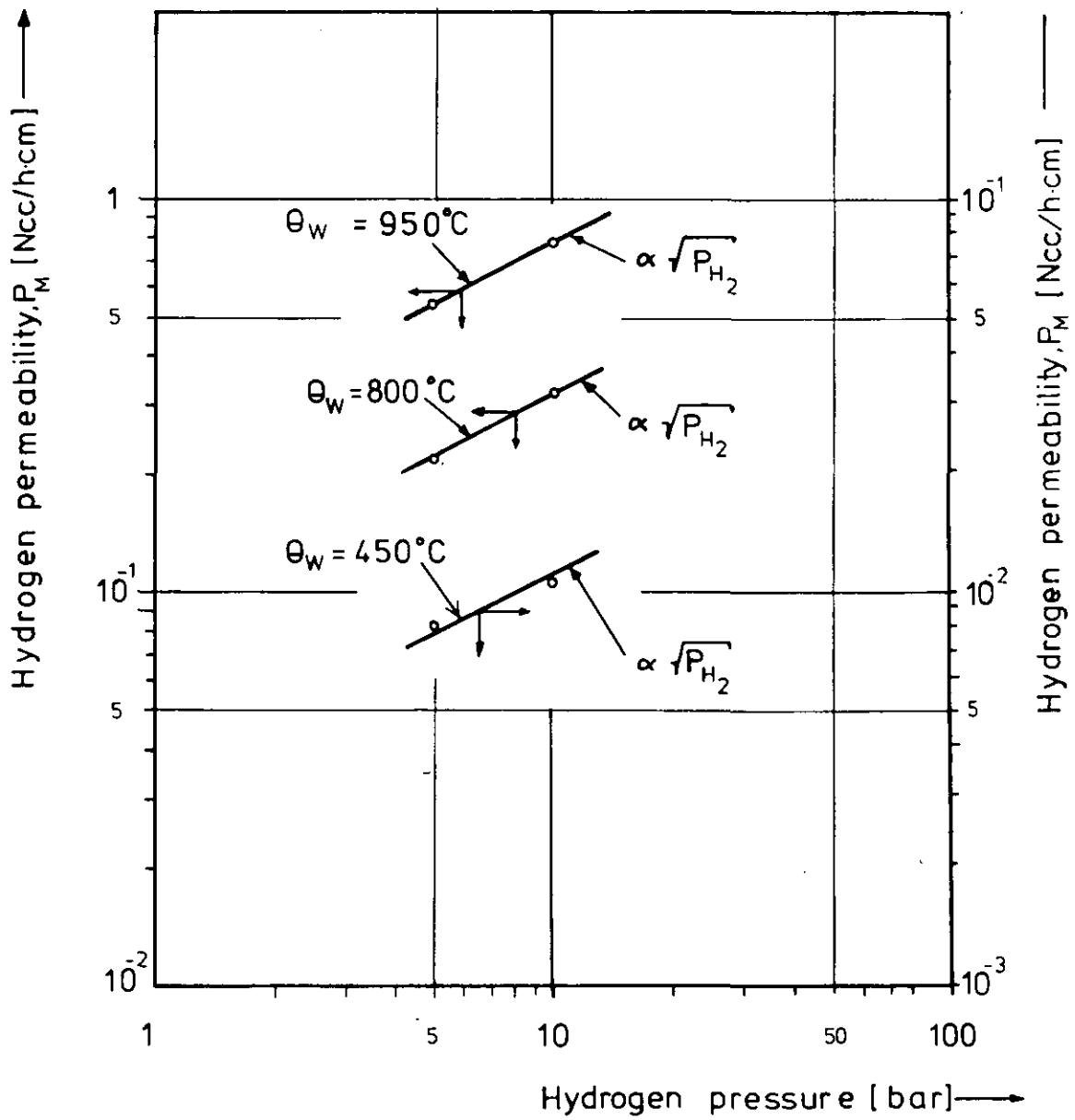


Figure 3.2 The dependency of hydrogen permeation on hydrogen pressure (material: Incoloy-800)

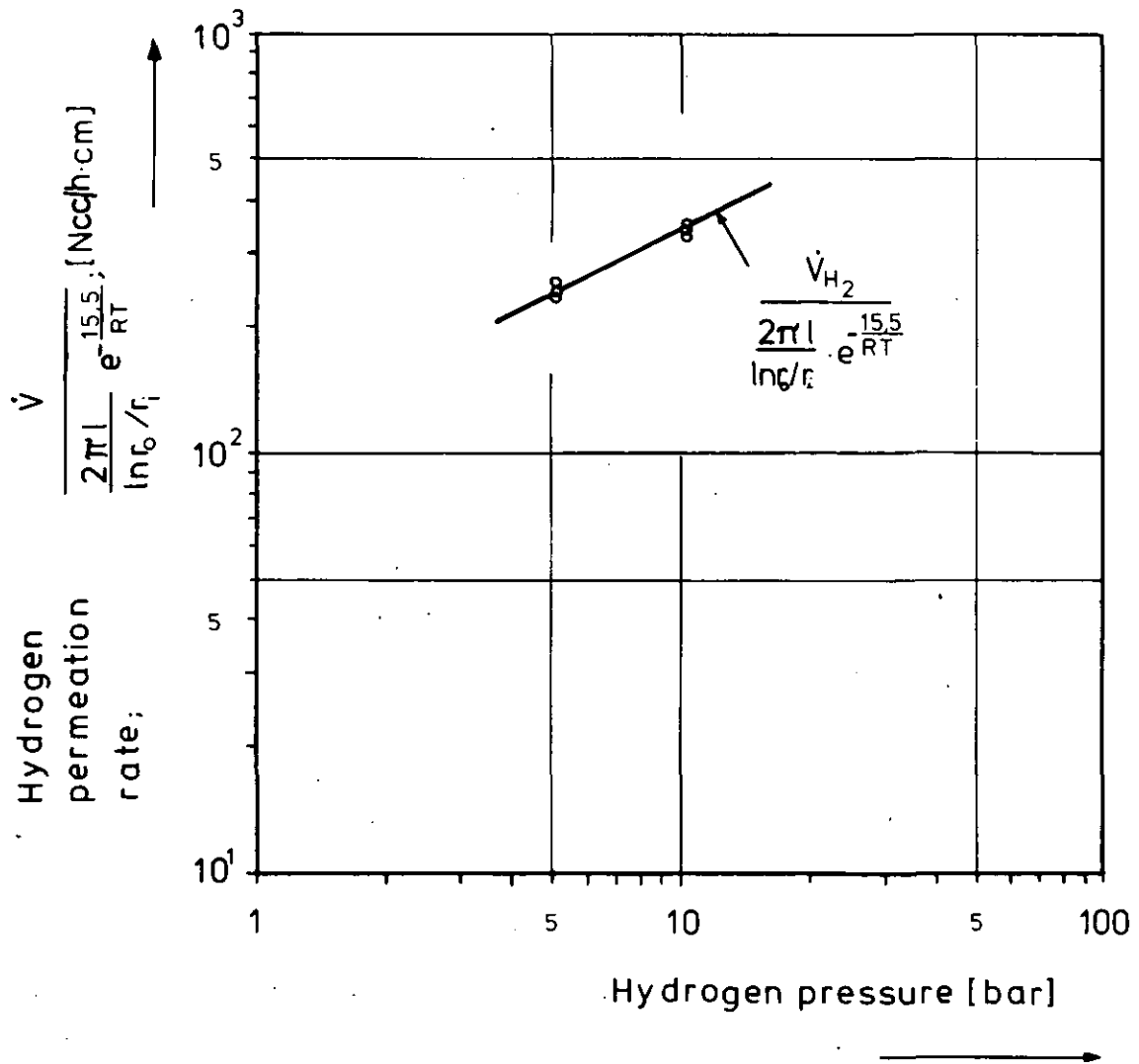


Figure 3.3

The dependency of hydrogen permeation on hydrogen pressure (material: Incoloy-800)

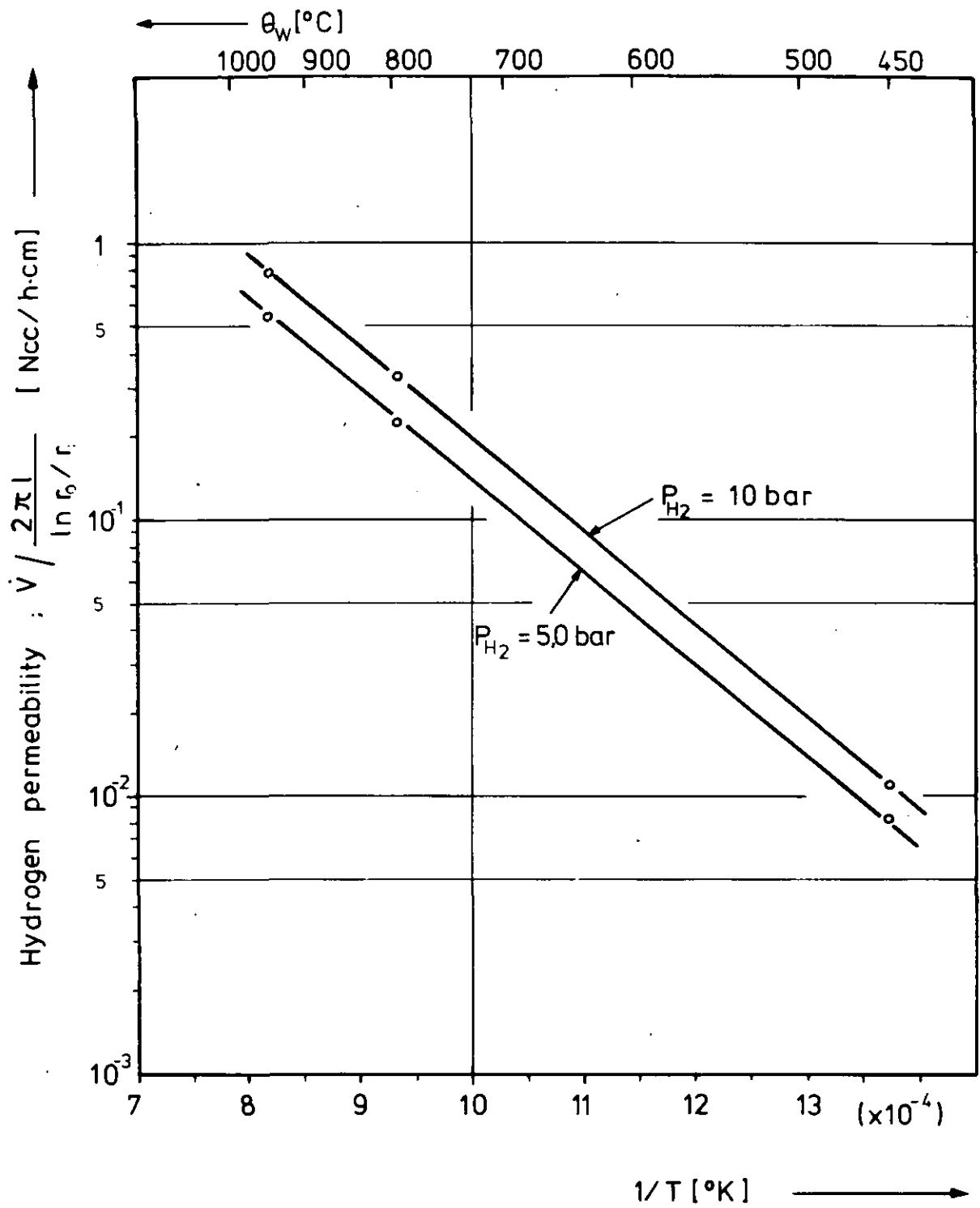


Figure 3.4 The relation between hydrogen permeability and sample temperature

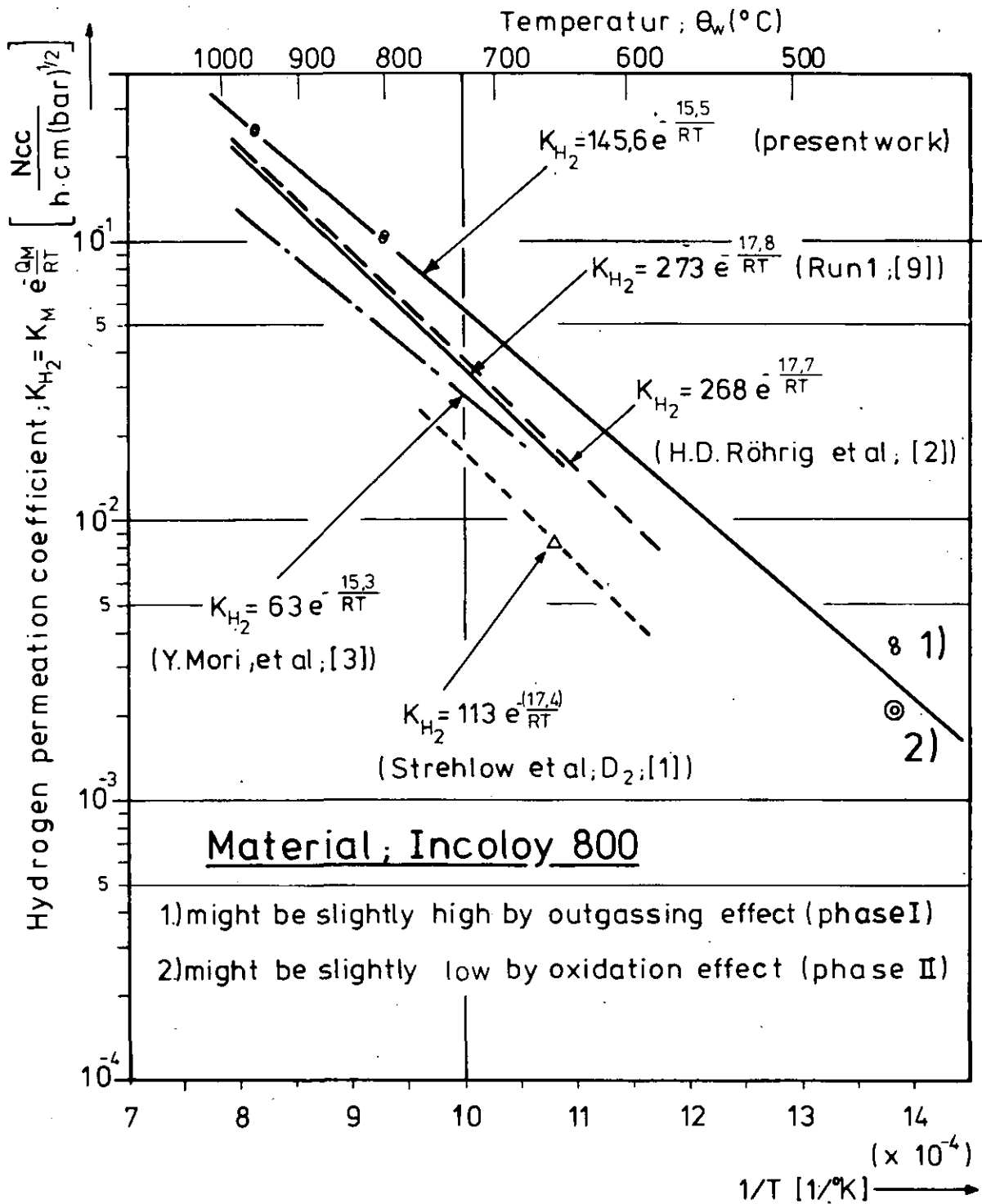


Figure 3.5

The dependency of the hydrogen permeation coefficient on the sample temperature (Arrhenius plot of the permeation coefficient)

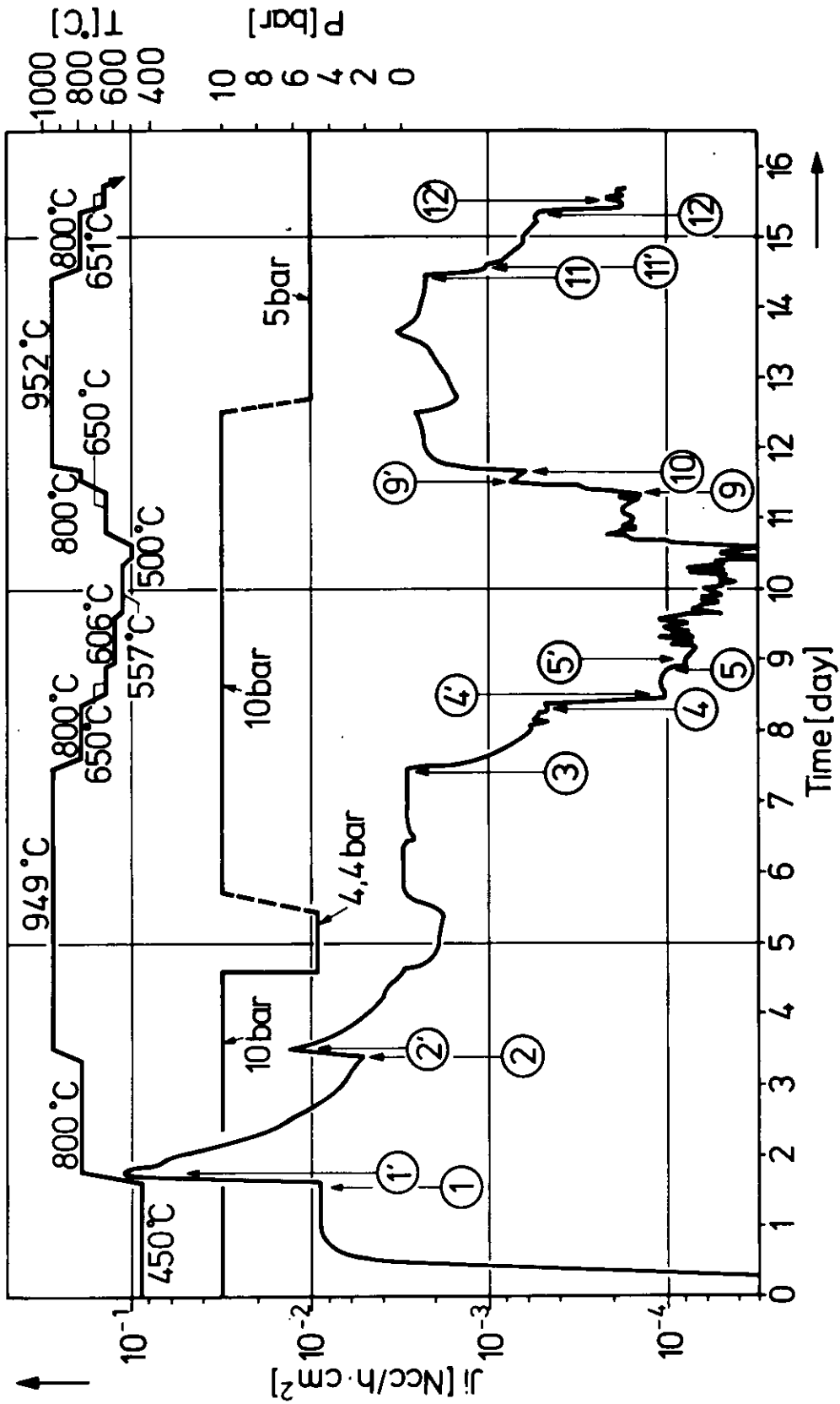


Figure 3.6 Measured hydrogen permeation flux (test sample 106)

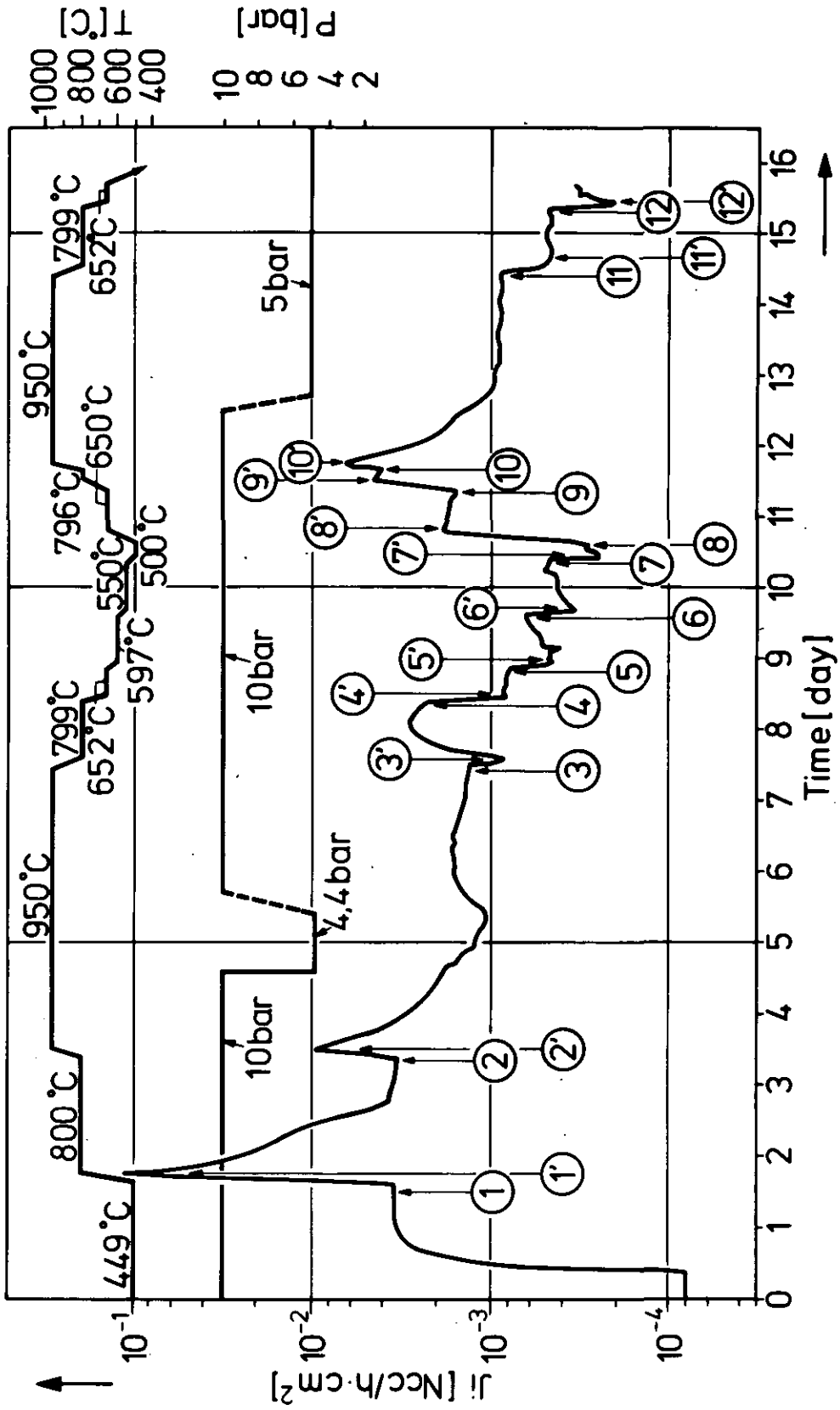


Figure 3.7 Measured hydrogen permeation flux (test sample 1o7)

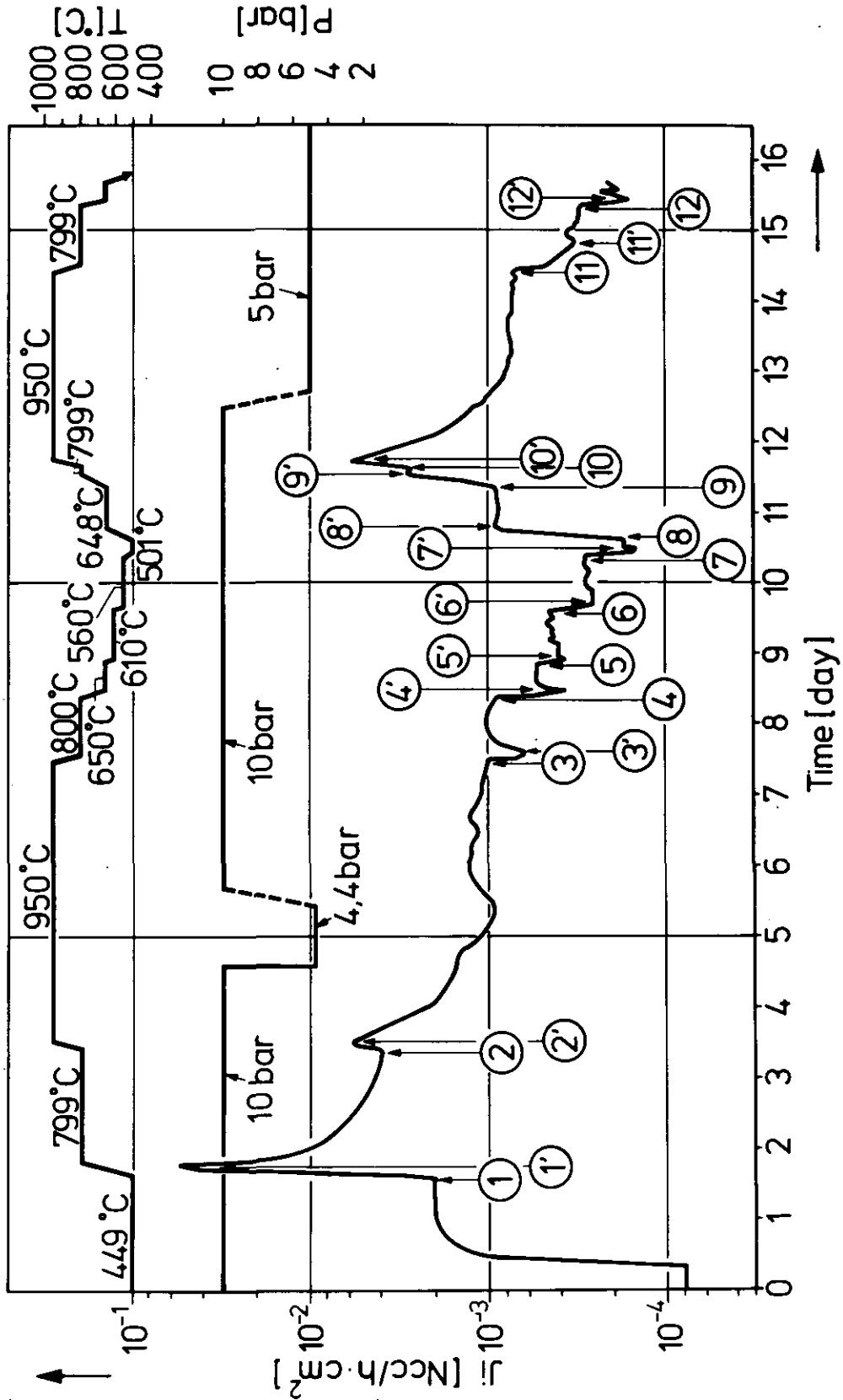


Figure 3.8 Measured hydrogen permeation flux (test sample 1o8)

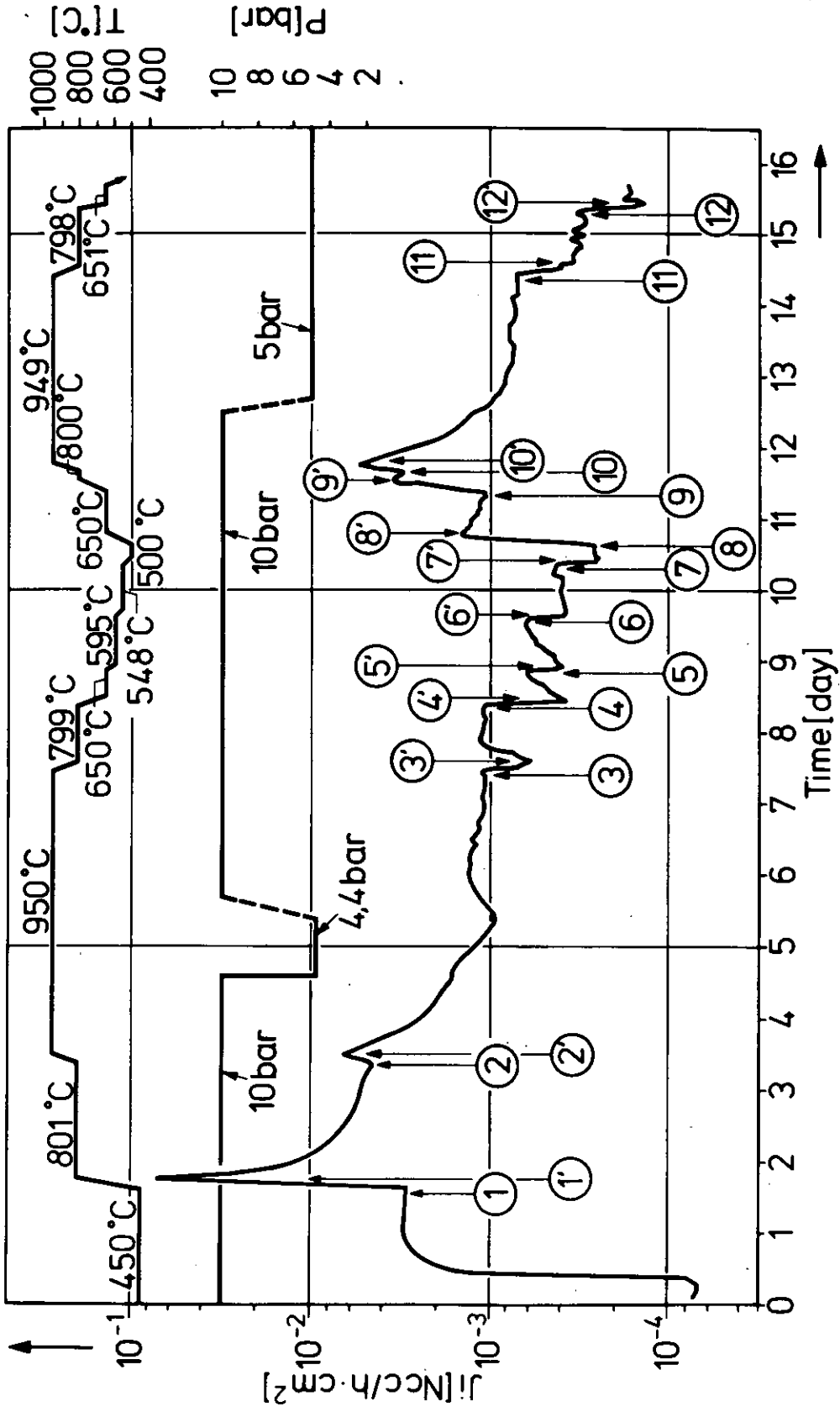


Figure 3.9 Measured hydrogen permeation flux (test sample 109)

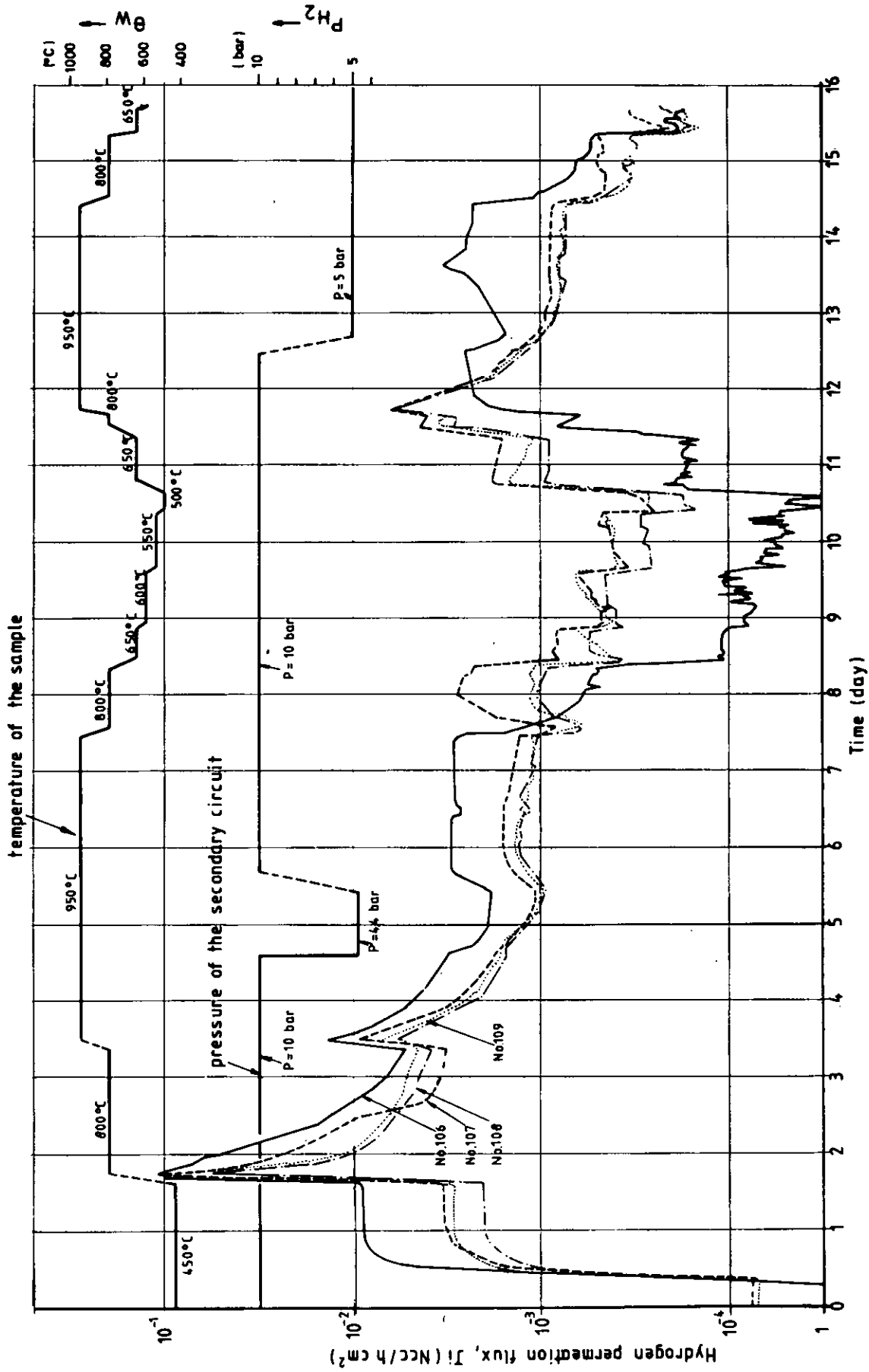


Figure 3.10 Comparison of the hydrogen permeation rate between 4 test samples

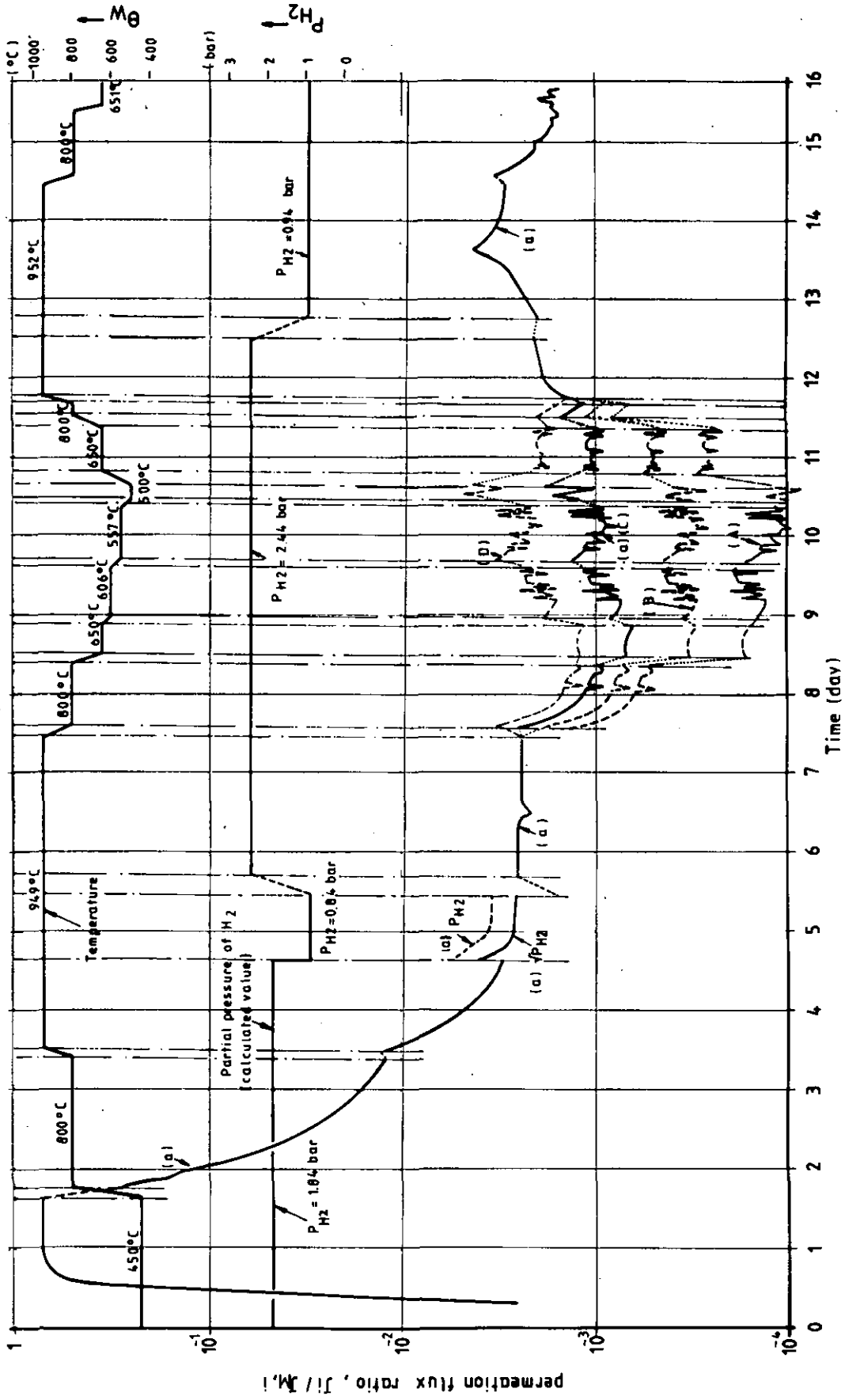


Figure 3.11 Hydrogen permeation flux ratio, $J_i/J_{M,i}$ (test sample 106)

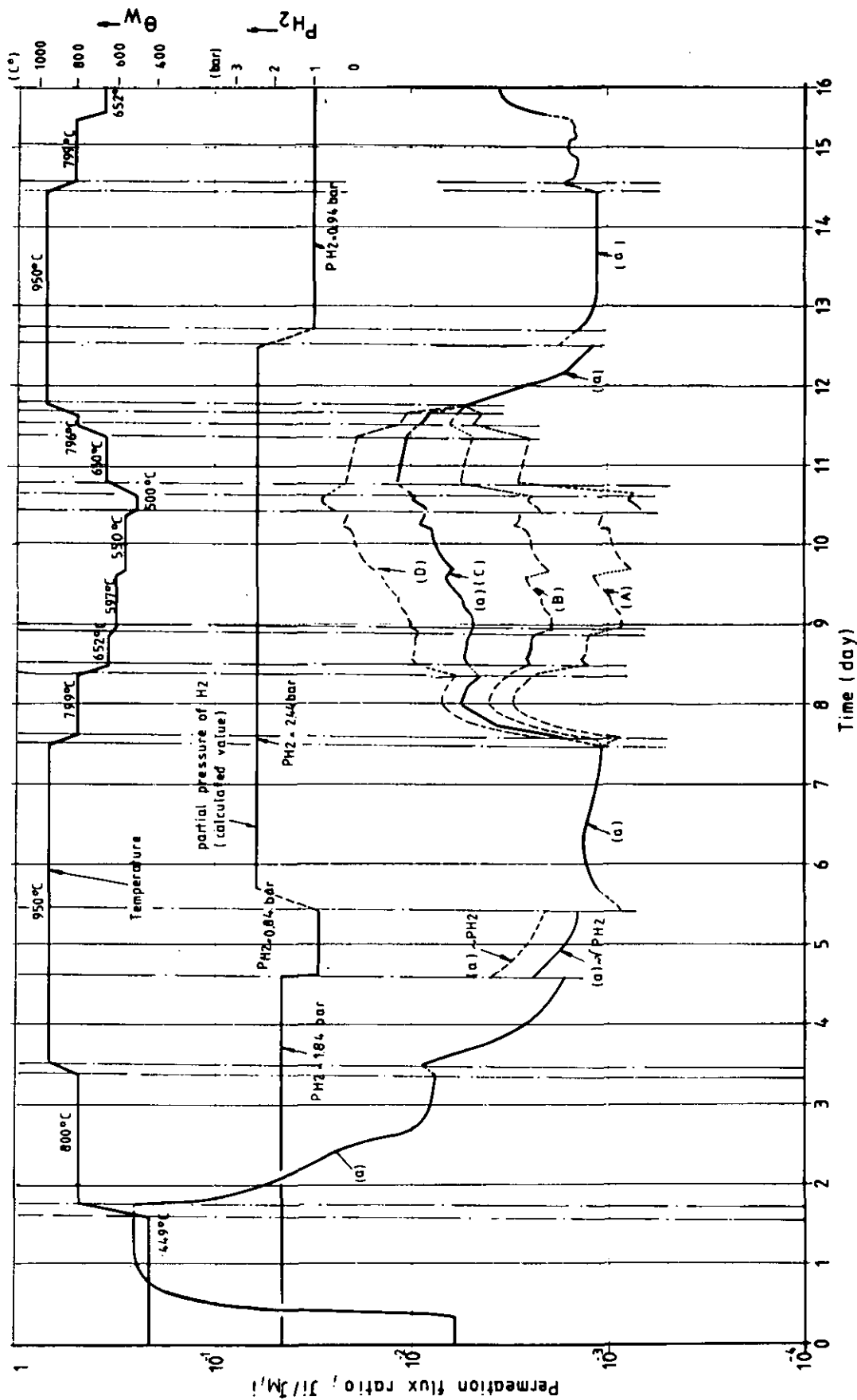


Figure 3.12 Hydrogen permeation Flux ratio, $J_i/J_{m,i}$ (test sample 107)

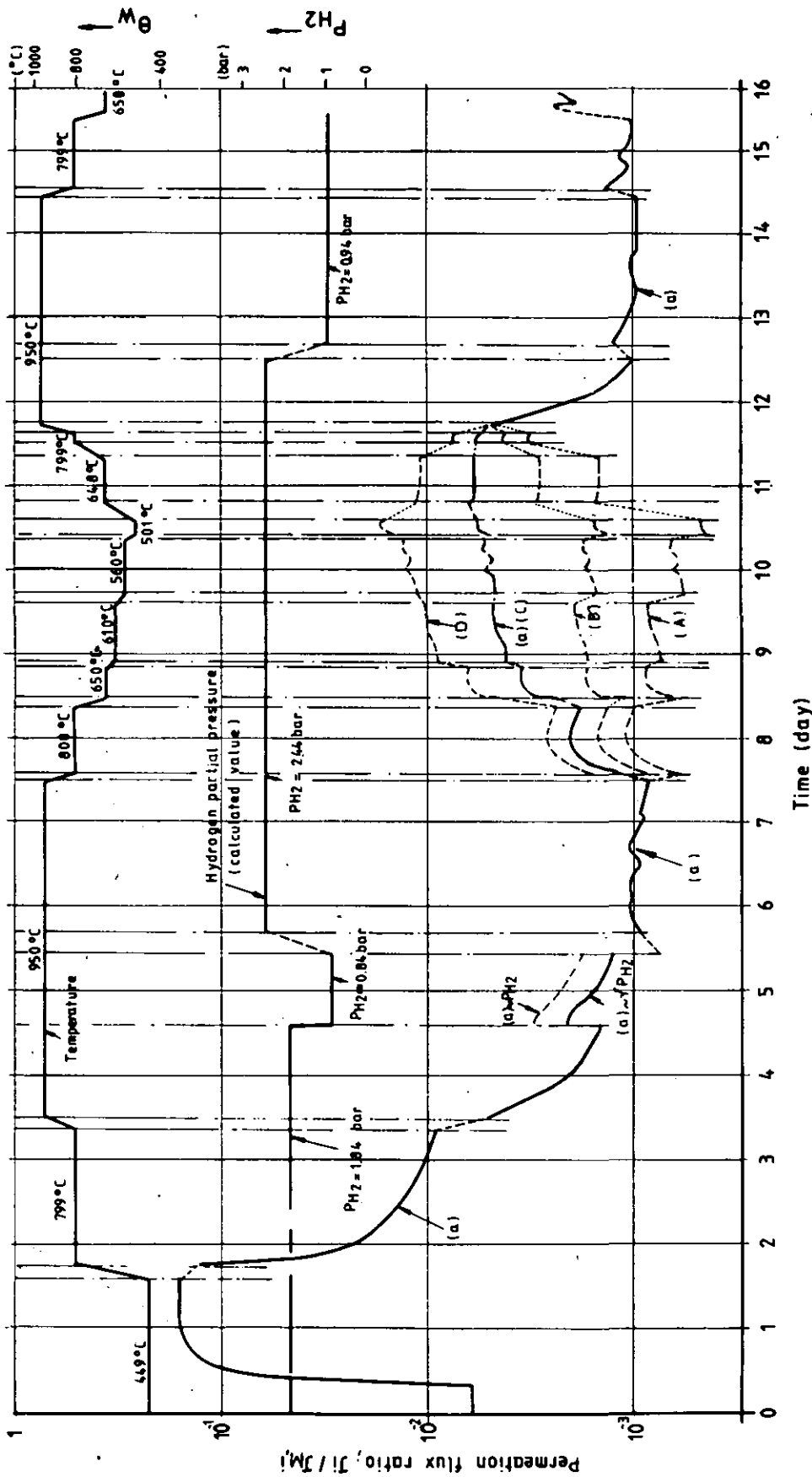


Figure 3.13 Hydrogen permeation flux ratio, $J_i/J_{M,i}$ (test sample 108)

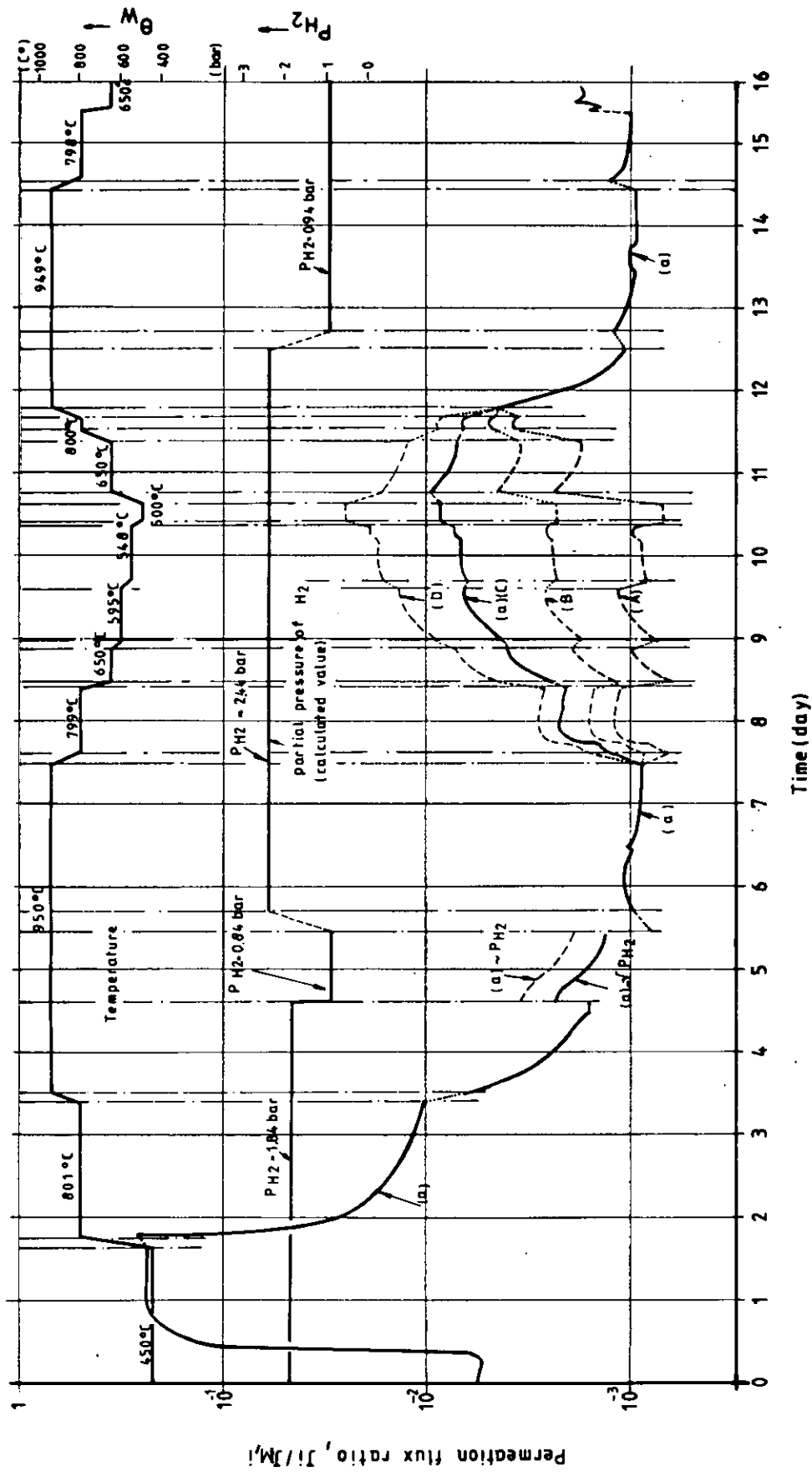


Figure 3.14 Hydrogen permeation flux ratio, J_1/J_{M1} (test sample 109)

Table III Temperature changing speed

Test sample No. 106

Temperature change	Temperature changing speed
949 → 800 ^o C	170 ^o C/h
800 → 650 ^o C	130 ^o C/h
650 → 606 ^o C	70 ^o C/h
606 → 557 ^o C	70 ^o C/h
557 → 500 ^o C	60 ^o C/h
500 → 650 ^o C	60 ^o C/h
650 → 800 ^o C	70 ^o C/h
800 → 952 ^o C	110 ^o C/h
952 → 800 ^o C	170 ^o C/h
800 → 651 ^o C	130 ^o C/h

Test sample No. 107

Temperature change	Temperature changing speed
950 → 799 ^o C	170 ^o C/h
799 → 652 ^o C	130 ^o C/h
652 → 597 ^o C	70 ^o C/h
597 → 550 ^o C	70 ^o C/h
550 → 500 ^o C	60 ^o C/h
500 → 650 ^o C	60 ^o C/h
650 → 796 ^o C	70 ^o C/h
796 → 950 ^o C	110 ^o C/h
950 → 799 ^o C	170 ^o C/h
799 → 652 ^o C	130 ^o C/h

Test sample No. 108

Temperature change	Temperature changing speed
950 → 800 ^o C	170 ^o C/h
800 → 650 ^o C	130 ^o C/h
650 → 610 ^o C	70 ^o C/h
610 → 560 ^o C	70 ^o C/h
560 → 501 ^o C	60 ^o C/h
501 → 648 ^o C	60 ^o C/h
648 → 799 ^o C	70 ^o C/h
799 → 950 ^o C	110 ^o C/h
950 → 799 ^o C	170 ^o C/h
799 → 650 ^o C	130 ^o C/h

Table III. Temperature changing speed (continued 1)

Test sample No. 109

Temperature change	Temperature changing speed
950 → 799 ^o C	200 ^o C/h
799 → 650 ^o C	150 ^o C/h
650 → 595 ^o C	70 ^o C/h
595 → 548 ^o C	70 ^o C/h
548 → 500 ^o C	60 ^o C/h
500 → 650 ^o C	60 ^o C/h
650 → 800 ^o C	70 ^o C/h
800 → 949 ^o C	110 ^o C/h
949 → 798 ^o C	200 ^o C/h
798 → 651 ^o C	150 ^o C/h

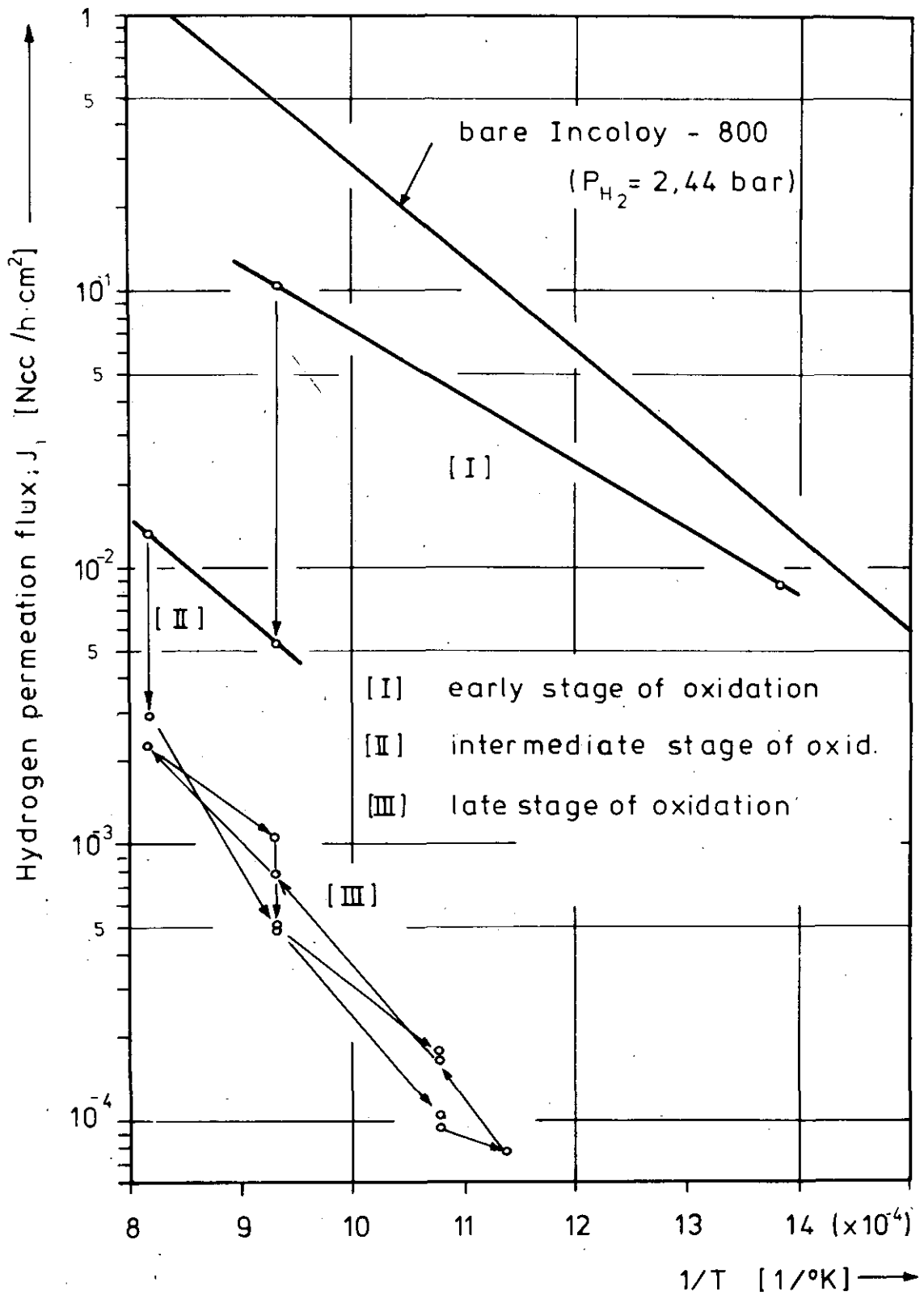


Figure 3.15 The effect of temperature and time during the exposure of the process gas (Test sample 106)

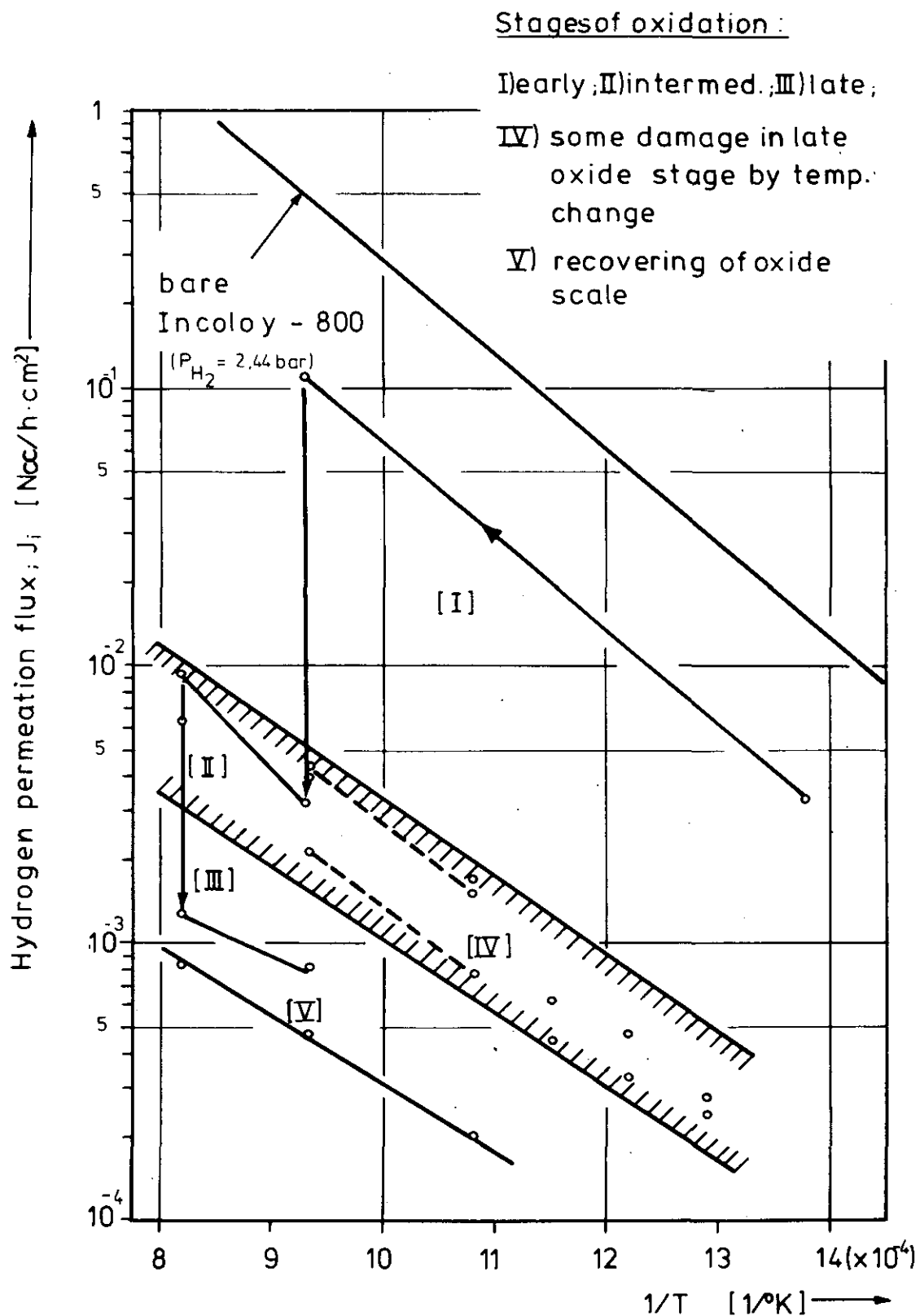


Figure 3.16 The effect of temperature and time during the exposure to the process gas (test sample 1o7)

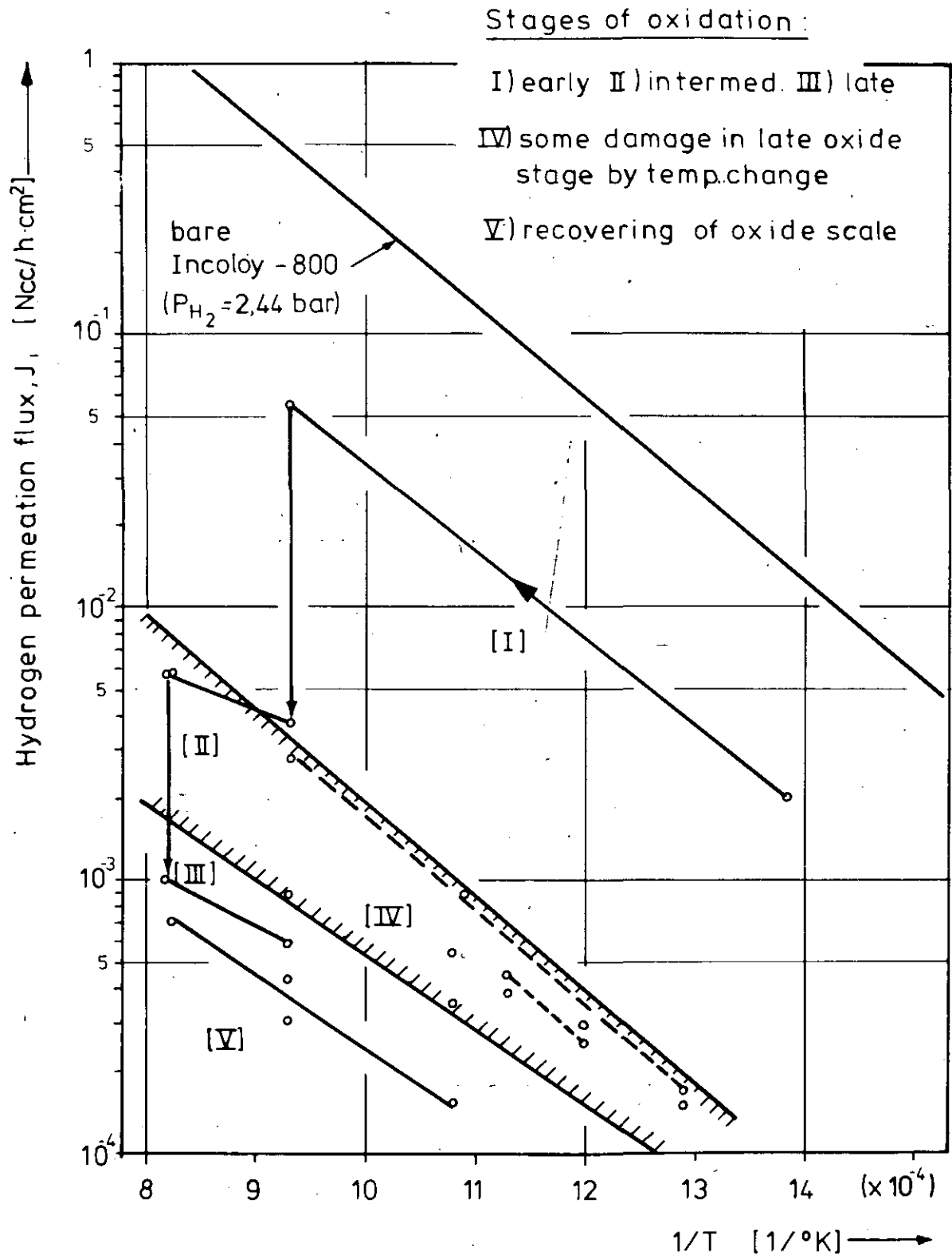


Figure 3.17 The effect of temperature and time during the exposure to the process gas (Test sample 1o8)

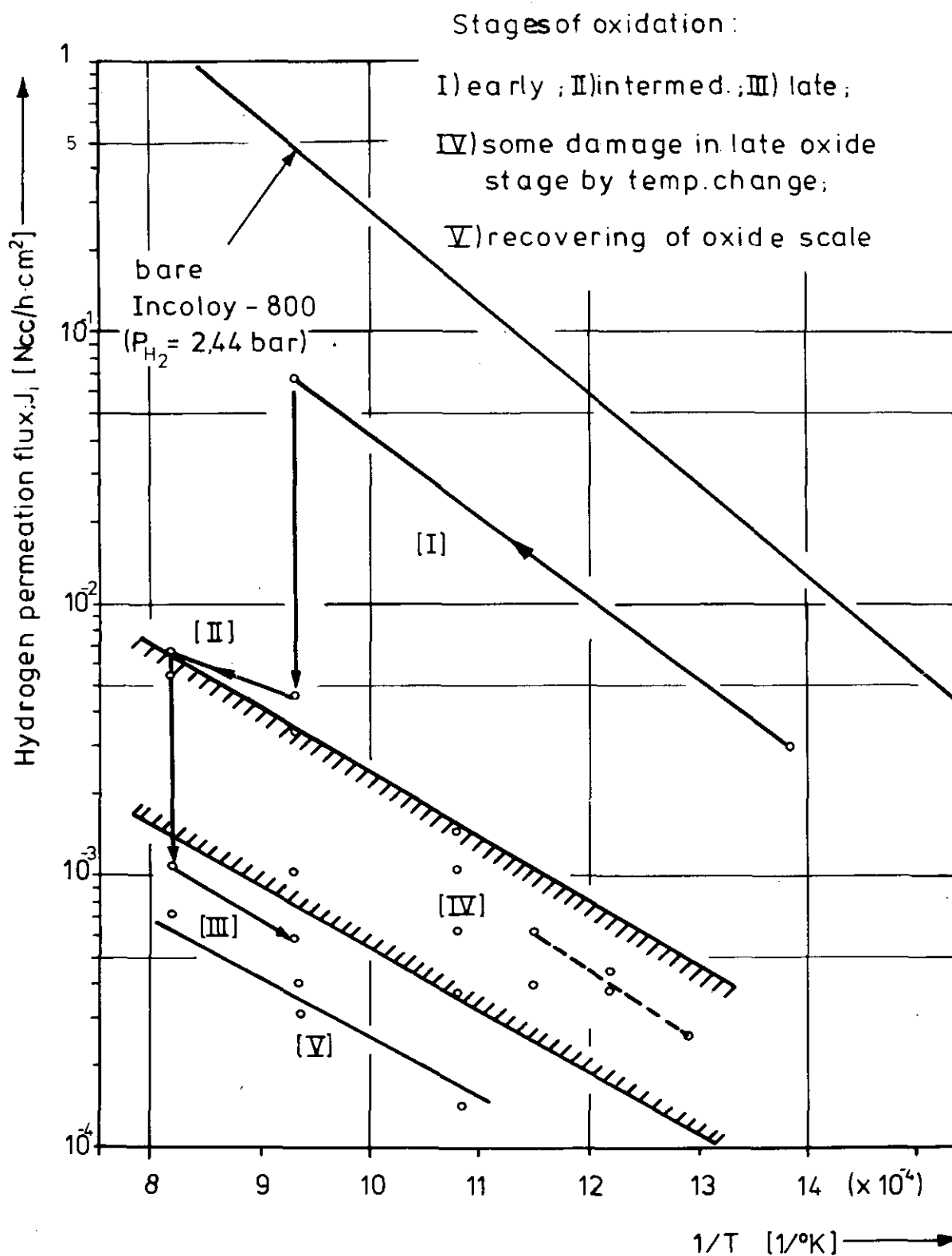


Figure 3.18 The effect of temperature and time during the exposure to the process gas (Test sample 109)

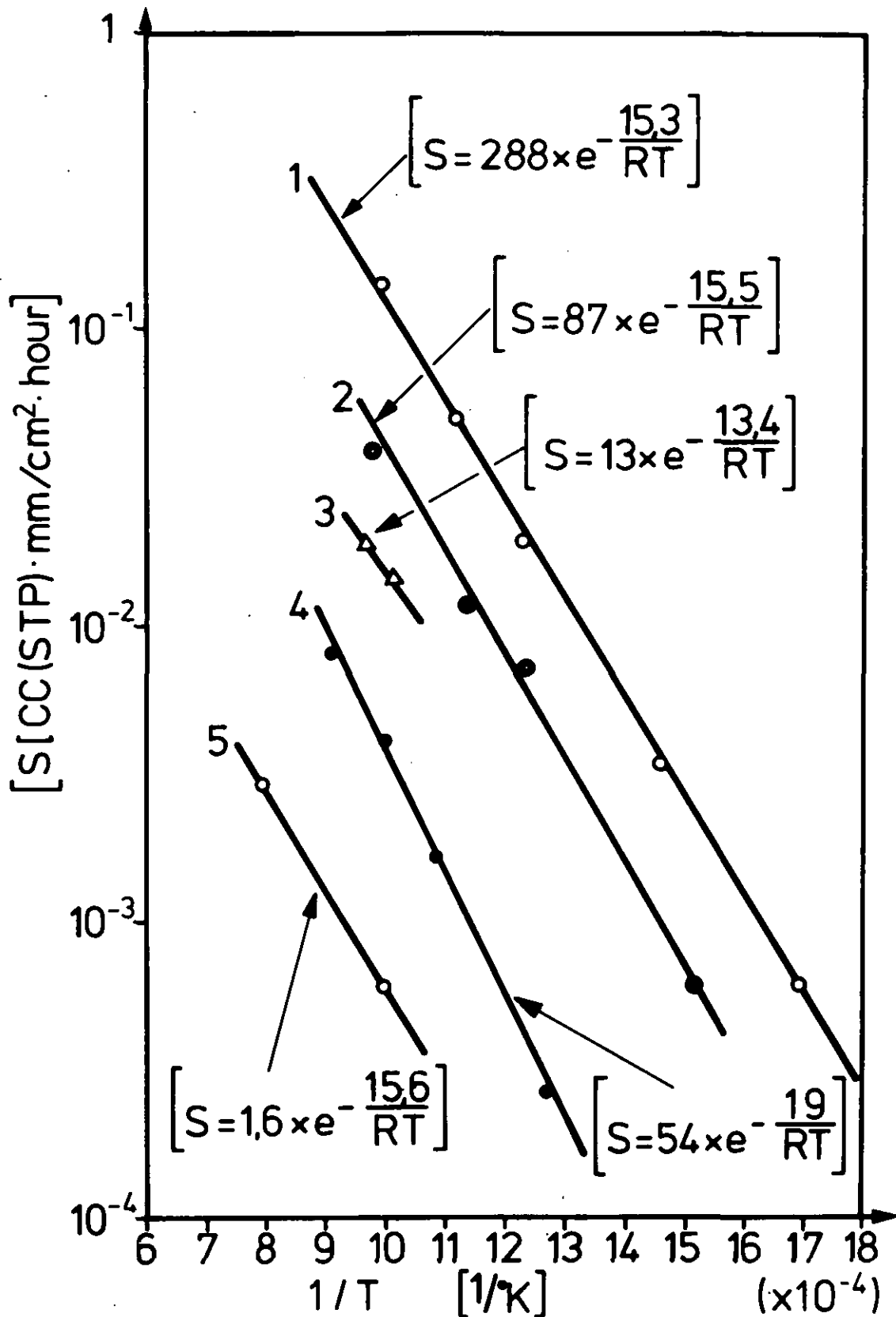


Figure 3.19 The comparison of activation energies between 347 stainless steels treated by various methods ⁽¹⁰⁾.

Figure 3.19 (complement)

curve 1; bare 347 s.s.
 curve 2; 347 s.s. coated by No.32 coating material +
 exposed to wet H_2 at $1000^{\circ}C$ for 1 hour.
 curve 3; 347 s.s. coated by No. 418 coating material
 curve 4; 347 s.s. coated by No. 327 coating material
 curve 5; 347 s.s. oxidated in wet H_2 at $979^{\circ}C$ for
 3 hours .

composition of 347 stainless steel

Fe	Cr	Ni	Mn	Ta	c
68.1%	18.4%	13.3%	0.4%	<0.1%	0.08%

oxides contained in coating materials (see ref. (10))

coating material No.32;	SiO_2 , Al_2O_3 , Na_2O K_2O , NiO , MnO_2 B_2O_3 , CaF_2
coating material No.327;	SiO_2 , Al_2O_3 , Na_2O K_2O , V_2O_5 , FeO
coating material No. 418;	Cr_2O_3